UNIVERSITY OF CALIFORNIA SAN DIEGO

Neuronal inactivity induces the post-stroke critical period through NR2B-dependent synaptic modifications in mice

A dissertation submitted in partial satisfaction of the
requirements for the degree Doctor of Philosophy

in

Biomedical Sciences

by

Eric Wang

Committee in charge:

Professor Byungkook Lim, Chair
Professor Davide Dulcis
Professor William Joiner
Professor Mark Tuszynski
Professor Binhai Zheng

2021

The Dissertation of Eric Wang is approved, and it is acceptable in quality and form for publication on microfilm and electronically.

University of California San Diego

2021

DEDICATION

For Grandma, Grandpa, Shima and everyone who helped me succeed

EPIGRAPH

What does it mean to understand an elephant?

John Krakauer

TABLE OF CONTENTS

LIST OF FIGURES

ACKNOWLEDGMENTS

My path to my doctoral degree does not begin with my admission to graduate school or even college. If anything, it begins with the culture of intellectual freedom and unconditional love and support that my grandparents (great grandparents?) have made the bedrock of my family. The word “grateful” does not do justice to the years of support and sacrifice that they have made. Along my path, I have lost many members of my family, but I like to think that I have and will continue to pass on this culture – this spirit of kindness and adventure – to future generations.

Just as science is not done in isolation, my successes cannot only be attributed to me and my family. I have been fortunate to have made the right friends who kept me on the right path, who motivated me to work harder, and to support me wholly. Shout outs to Amanda Tran, Shyam Srinivasan, Harold Pan, Alton Ng, Carolyn Chuang, Jennifer Uren, Kevin Wang, Pai-Kai Huang, Kyle Rentschler, Heidi Ho, Janet Lee, Ipshita Zutshi, Varoth Lilascharoen, Daniel Knowland, Stefan Pate, Jun-Hyeok Choi, Qing-Di Wang, Christopher Yoon, Russell Ro and many others.

Intellectually, I am also grateful to the continued support of my undergraduate mentors – Drs Milton Saier and Russell Doolittle – who opened the door to my research careers and the many scientists who have continued to open doors for me: Gary Steinberg, Tonya Bliss, Ahmet Arac, Nate Manley, Derek Reubish, Takeshi Hiu, Yasuhiro Nishiyama, Takuma Wakai, Shunsuke Ishizaka, Masaki Ito, Guohua Sun, Jenny Ross, Paul George, Davide Dulcis, Binhai Zheng, Mark Tuszynski, and William Joiner.

But perhaps beyond everyone else, I am entirely indebted to Michelle Cheng and Byungkook Lim who took an exceptional risk in giving me a chance to work with them. With their mentorship, I was able to really refine my science, my thinking, and my personal values of what really matters in life. They gave me the intellectual and experimental freedom to explore the far

reaches of neuroscience and have contributed greatly to the development of my project. Scientific coffee talks and texting ideas at all hours of the night are some of my fondest memories that I will always cherish. Thank you.

Chapter 1 - 3, in full, is currently being prepared for submission for publication of the material. Wang, Eric; Lilascharoen, Varoth; Wang, Qingdi; Tran, Amanda; Yoon, Christopher; Honma, Patrick; Shu, Senling; Ro, Russell; Choi, Jun-Hyeok; Wang, Xiao-Yun; Knowland, Daniel; Lim, Byungkook. The dissertation author was the primary investigator and author of this material.

VITA

2011	Bachelor of Science in Physiology & Neurosciences, UC San Diego
2012-2015	Life Science Research Associate, Stanford University
2019	Instructional Assistant, UC San Diego
2021	Doctor of Philosophy in Biomedical Sciences, UC San Diego

PUBLICATIONS

Lilascharoen V*, Wang EH*, Do N, Pate S, Tran AN, Wang XY, Park YG, Chung KH, BK Lim. Divergent pallidal pathways underlying distinct Parkinsonian behavioral deficits (Nature Neuroscience. 2021 Mar 15)

Pendharkar AV, Smerin D, Gonzales L, Wang EH, Levy S, Wang S, Ishizaka S, Ito M, Uchino H, Chiang T, Cheng MY, Steinberg GK. Optogenetic stimulation reduces neuronal nitric oxide synthase expression after stroke (Trans Stroke Res. 2020 Jul 13)

Hwang EJ, Link TD, Hu YY, Lu S, Wang EH, Lilascharoen V, Aronson S, O'Neil K, Lim BK, Komiyama T. Corticostriatal flow of action selection bias (Neuron. 2019 Dec 18)

Keller JA, Chen J, Simpson S, Wang EH, Lilascharoen V, George O, Lim BK, Stowers L. Brainstem control of urethral sphincter relaxation and scent marking behavior (Nature Neuroscience. 2018 Aug 13)

Ito M, Aswendt M, Lee A, Ishizaka S, Cao Z, Wang EH, Levy S, Smerin D, McNab J, Zeineh M, Leuze C, Goubran M, Cheng MY, Steinberg GK. RNA sequencing analysis revealed a distinct motor cortex transcriptome in spontaneously-recovered mice after stroke (Stroke. 2018 Sept 1)

Knowland D, Lilascharoen V, Pacia C, Shin S, Wang EH, Lim BK. Distinct ventral pallidal neural populations mediate separate symptoms of depression (Cell. 2017 July 30)

Shah A, Ishizaka S, Cheng MY, Wang EH, Bautista AR, Sun GH, Steinberg GK. Optogenetic stimulation of the cerebellar dentate nucleus to promote functional recovery after stroke (Sci Reports 2017 Jun 1)

Hiu T, Farzampour Z, Paz J, Wang EH, Smith S, Huggenard J, Steinberg GK. Enhanced phasic GABA inhibition during the repair phase of stroke: a novel therapeutic target (Brain. 2015 Dec 18)

Wakai T, Narasimhan P, Sakata H, Wang EH, Chan PH. Hypoxic preconditioning enhances neural stem cell transplantation therapy after intracerebral hemorrhage in mice (Journal of Cerebral Blood Flow and Metabolism. 2015 Oct 27)

Cheng MY, Wang EH, Steinberg GK. Optogenetic approaches to study stroke recovery. (American Chemical Society Neuroscience. 2014 September 26)

Cheng MY, Wang EH, Woodson WJ, Wang S, Sun GH, Lee AG, Arac A, Fenno LE, Deisseroth K, Steinberg GK. Optogenetic neuronal stimulation promotes functional recovery after stroke. (Proc Nat Acad Sci. 2014 August 18)

Shlykov M, Zheng BH, Wang EH, Saier M. Transmembrane molecular transporters facilitating export of molecules from cells to organelles. (Microbial efflux pumps: current research. 2013; 1-20)

ABSTRACT OF THE DISSERTATION

Neuronal inactivity induces the post-stroke critical period through NR2B-dependent synaptic modifications in mice

by

Eric Wang

Doctor of Philosophy in Biomedical Sciences

University of California San Diego, 2021

Professor Byungkook Lim, Chair

The reestablishment of functional neural networks is vital to stroke recovery and readily occurs during the post-stroke critical period: a window of heightened neuroplasticity and training sensitivity. Although evidence suggests that neural repair processes are engaged as a part of the obligate response to stroke, the mechanisms of these processes remain unknown. Here, using widefield and 2-photon calcium imaging of awake, behaving mice, we determined that surviving neurons in the perilesional tissue are inactive after stroke. These neurons adapt to this prolonged inactivity after stroke by modifying excitatory synapses to include more NR2B-containing NMDA receptors. The inactivity-mediated increase in NR2B expression is critical for recovery since

NR2B antagonism or chemogenetic activation prevents recovery. We also demonstrate that experimental neuronal inactivation can restore the post-stroke critical period in a NR2B-dependent manner. Together, our results identify a novel potential stroke therapy and provide a conceptual framework for post-stroke plasticity and functional recovery.

INTRODUCTION

Stroke remains a leading cause of adult disability in the entire world. Despite decades of research, billions of research dollars and the extreme personal and societal costs that come from having a stroke, we do not have a drug to treat stroke. Until recently, the sole focus of translational stroke research has been on neuroprotection: reducing the progression of ischemic stroke. However, hundreds of clinical studies into these compounds have largely failed, and thus, the field is now focusing on stroke recovery: promoting the reacquisition of lost function. I am skeptical of the efficacy of drugs alone to promote stroke recovery.

Our current understanding of neuroscience and how the brain generates animal behaviors is premised on the idea that the pattern of muscle fiber contractions that we call a behavior emerges from the flow of electrical activity through intricately wired neural circuits. To some degree, the configuration of these neural circuits is innate, but it is evident that development and experiences play a large role in shaping the configuration of these circuits. Learning is the process of reorganizing neural circuits to achieve better behavioral performance[8]. On the other hand, brain injuries such as stroke, damages these neural circuits, impairs the flow of information to muscle fibers, and impairs animal behaviors. And thus, functional recovery must require the re-establishment of some configuration of neural circuits that can generate the appropriate pattern of muscle fiber contraction.

It is with this in mind that I am so skeptical about the sufficiency of drugs to promote stroke recovery. It is unclear to me how drugs alone can recapitulate the intricacies of neural wiring. By contrast, we know that learning is the process of rewiring neural circuits to achieve better behavioral performance, so *motor learning* should be able to rewire the surviving neurons into new functional circuits that can perform the task (eg. functional recovery) [1,2,7]. Indeed, early

rehabilitative training has been shown to effectively promote recovery across a variety of animal species after brain injuries. By early, I mean that if one were to initiate rehabilitative training months or years after having a stroke, then its unlikely that one would make substantial functional gains; by contrast, initiating training weeks after stroke, and its much more likely for the patient to recover. This time-limited efficacy of rehabilitative training posits two models of post-stroke plasticity: 1) stroke temporarily makes the brain much more plastic, and 2) the brain becomes increasingly less plastic after stroke[1,2,7].

Much of the previous decades of research on gene expression profiling and cellular characterizations suggests that stroke does indeed make the surviving neurons much more plastic. However, only recently was this idea clearly demonstrated through a very clever experiment by Steve Zeiler and Jon Krakauer[1,2,7]. The idea is as follows: if stroke does make the surviving neurons more plastic, then inducing a second stroke after the transient period of heightened training sensitivity should restore training sensitivity and provide subjects an additional opportunity to undergo rehabilitative training and recover from stroke. Using a mouse model of stroke, they showed that this indeed was the case: that a second stroke restores training sensitivity[1,2,7]. Obviously, inducing a second stroke in human patients is ethically unviable, and thus, we desperately need a functional alternative. I speculate that if we were to understand the mechanisms by which stroke induces a period of heightened training sensitivity, then we might be able to trick the brain into thinking it's been injured without actually doing so. And thus, we must understand how the brain responds to stroke. Indeed, understanding how the brain adapts to brain injuries, such as stroke, can have profound implications for the treatment of neurological diseases; yet little is known about the trigger and substrate of these adaptations[1-6]. That stroke induces this "post-stroke critical period" suggests that an enhanced plastic state may be a part of the obligate response

to injury[3]. And therefore, discovering how damage can induce the post-stroke critical period may inspire new therapeutic approaches to extend or even restore this plastic state and provide patients additional opportunities to recover.

The traditional perspective toward understanding biological processes is that of an open-loop system: a sequence of biochemical reactions. To be concrete, consider the hypothesis that neurons and neural circuits adapt to injuries by transiently becoming much more plastic[3]. This implies that neurons and neural circuits possess a means to *detect* when it has been injured; in response to this "injury signal", neurons and neural circuits activate repair processes that make the system much more plastic. And so, this open-loop perspective, raises several intriguing questions: 1) what is the injury signal, 2) what mechanisms detect this signal, 3) what cellular and molecular processes are activated in response to detection of the injury signal, and 4) which of these processes contribute to the state of heightened neural plasticity.

It is worth mentioning that a highly plastic state is not without drawbacks; if a system is too plastic, it is unlikely to be able to retain memories or acquired patterns for long periods of time. This can be incredibly deleterious for the survival of an animal – especially in the context of the nervous system where "forgetfulness" decreases the chances of survival. And therefore, it stands to chance that the system also has a means to reduce plasticity when the injury or perturbation ceases to be problematic. Therefore, I speculate that the open-loop perspective is only part of the story. The critical missing component is feedback signal the indicates when the injury has been resolved and incorporation of this negative feedback signal effectively "closes the loop" in the same way that a thermostat is a closed-loop system. And just as in the thermostat, there must exist a means to detect the signal (eg. thermometer), a process that is activated in response to extreme perturbations (eg. turning on the A/C), and a setpoint that the system tries to maintain (eg. 72^{o}F).

Viewing the problem from this closed-loop perspective raises several additional questions such as 1) what is the negative feedback signal, 2) what are the processes that activated or inactivated as a result of this signal, and 3) how much of a lag between the detection of this feedback signal and when the processes are activated/inactivated. Moreover, an important feature of negative feedback systems is the idea of a "setpoint" or a dynamic range of values that the system tries to maintain; perturbing the system outside of this range triggers mechanisms that bring the system back to the normal dynamic range. And thus, subsequently interesting questions are: 1) what is/are the variable(s) that are being optimized, 2) what are the components that sets the setpoint, 3) how much of a dynamic range exists around this point. Here, we consider what we believe to be the two most quintessential questions: 1) what is the "injury" signal, 2) what processes are activated in response to this injury signal. Using the thermostat as an exemplar, we speculate that the injury resolved signal emerges from the processes activated by the injury signal. To gain insight into the answers to these questions, we constrained our search to processes that contribute to a state of heightened neural plasticity.

Synaptic plasticity is one of the most canonical forms of neural plasticity. Synaptic plasticity can be achieved through several molecular and cellular implementations: by changing the number, the shape, the size, the location of synapses, and the molecular composition of synapses. Of note, these implementations can be regulated by both biochemical and bioelectricity. That is, high frequency activity of excitatory synapses leads to the depolarization of the postsynaptic membrane, which, in turn, removes the magnesium block of NMDARs and enables Ca^{2+} influx. High concentrations of Ca^{2+} initiates a cascade of intracellular signaling events that leads to substantial synaptic potentiation such as the incorporation of AMPAR into the

postsynaptic membrane. In this way, synaptic plasticity can be summarized in a pithy line: high activity strengthens synapses.

When considering the processes that strengthen synapses, it is worth mentioning that other processes may interact with synaptic mechanisms, and thus, increase or decrease the propensity for plasticity (eg. potentiation or depression) to occur. For example, the co-incident activation of dopamine receptor (DRD1) with glutamate can more readily induce long term potentiation (LTP). Alternatively, the molecular subunit composition of synaptic proteins such as NMDAR can influence the propensity for synaptic potentiation. Indeed, pioneering studies have shown that the presence of NR2B subunits in N-methyl-D-aspartate receptors (NMDAR) have altered kinematics such that it remains open longer after binding glutamate, and thus allows in more Ca^{2+} per unit of glutamate and reduces the synaptic potentiation threshold and enhances synaptic plasticity[10,12,14]. And thus, we hypothesize that stroke may augment neural plasticity by changing the molecular composition of excitatory synapses to include more NR2B subunits[8-13]. Moreover, we posit that elevated levels of NR2B expression may be an important element of the reparative processes during the post-stroke critical period and contribute to the heightened sensitivity to training.

In support of this idea, the basal level expression of NR2B subunits in adult neurons is incredibly low; however, during the developmental critical period, NR2B subunits are enriched in neurons. Over the course of development, the presence of these subunits are replaced with that of NR2A subunits which have considerably faster kinetics, and thus, allow the passage of fewer Ca^{2+} ions. As such, the enrichment of NR2B expression in nascent neurons in early neurodevelopment or in neural stem cells of the adult hippocampus is, in part, responsible for the susceptibility of these neurons to undergo long-term potentiation induction by experimental protocols.

Intriguingly, the expression of the NR2B subunit occurs in an activity-dependent manner. That is, after prolonged periods of attenuated neural activity, neurons increase translation of the NR2B subunit. Impressively, this has been demonstrated to be able to be regulated at the single synapse level. That is, in response to prolonged inactivation of a single presynaptic terminal, its postsynaptic counterpart, but not that adjacent synapses, adapts by increasing the expression of the NR2B subunit. The incorporation of these NR2B subunits increases the propensity of LTP induction so that subthreshold currents readily induce synaptic potentiation. Since prolonged periods of attenuated neural activity upregulates NR2B expression, we hypothesize that stroke increases NR2B levels by inactivating surviving neurons[8,10].

Taking a step back to consider the (in)activity-dependent regulation of NR2B subunits, one can notice a negative feedback system. In response to prolonged periods of inactivity, neurons adapt by increasing its expression of the NR2B subunit. Incorporation of these subunits increases the likelihood for synaptic potentiation to occur at excitatory synapses and, thus, presumably restore neural circuit activity to baseline levels. At the risk of sounding teleological, as neural activity increases, NR2B subunits are downregulated to maintain neural activity within a range. One must wonder this mechanism also explains the developmental downregulation of NR2B subunits. Nevertheless, in this framework, bioelectrical activity is under homeostatic regulation. That is, electrical activity (whether it be membrane potential or calcium concentrations) is a variable that neural circuits actively regulate by increasing or decreasing the propensity for synaptic plasticity. Certainly the idea of homeostatic synaptic plasticity (homeostatic regulation of neural activity) is not a new one, nor is the idea of metaplasticity (plasticity of plasticity); however, here, we speculate whether these may be shared concepts: one way that neural circuits can regulate its activity is through metaplasticity.

Other means of homeostatic regulation of neural activity exists such as through multiplicative synaptic scaling. In this model, the strengths *all* of the excitatory synapses are scaled down (or up) by a single multiplicative factor in response to prolonged periods of activity/inactivity. The multiplicative scaling ensures that the relative synaptic strengths between synapses remain preserved. Presumably, this process saturates the amount of AMPAR present at the synapse and prevents further synaptic potentiation from occurring. That is, it prevents further learning from occurring. In this way, multiplicative upscaling (prevents learning) can be thought of as the opposite of metaplasticity (enhances learning), and thus, presents a paradox: how can neurons both enhance and prevent learning in response to prolonged periods of inactivity?

A recent paper suggests that different mechanisms are activated under different inactivity regimes. That is, in response to modest inactivity, neurons adapt through metaplasticity (overexpressing NR2B subunits); however, under extreme bouts of inactivity, neurons engage multiplicative scaling. And thus, it stands to reason that modest amount of inactivity might be able to activate metaplastic mechanisms, but extreme inactivity can prevent learning from occurring.

To summarize, our proposed closed-loop framework is as follows: stroke damage inactivates the surviving neurons - possibly through deafferentation; after a prolonged period of bioelectrical inactivity (injury signal), surviving neurons adapt by increasing its NR2B expression and induces a metaplastic reduction the synaptic potentiation threshold; coincident residual activity potentiates select synapses and restores activity to baseline levels. A key point here is that, unlike multiplicative scaling, not all synapses are potentiated – only specific synapses that are activated. This provides a state of heightened sensitivity to environmental experiences such as that of rehabilitative training – activating and potentiating the synapses that are implicated in moving / attempting to move. And thus, a standing question in the field is that of the “credit assignment

problem" or how does the brain specify which synapses to potentiate/depress in order to achieve better performance?

Regardless, an important first step towards testing our hypothesis is to demonstrate that surviving neurons are indeed inactive after stroke. However, both hypo- and hyperactivity are reported in the perilesional tissue after stroke[1,4,15,16]. This discrepancy may reflect the challenges in disambiguating the acute effects of stroke (e.g., deafferentation) and the chronic neural adaptations to these effects (e.g., homeostatic synaptic plasticity). Since neural adaptations likely contribute to functional recovery, a common strategy to separate the acute effects from the chronic adaptations is to compare the surviving tissue before and after recovery takes place[5]. However, many previous studies focus on training-induced recovery, which we argue is confounded by the fact that training itself, even without injury, modifies synaptic properties and alters neural activity[17-19]. Therefore, our approach begins by examining training-independent (i.e., spontaneous) recovery in mice.

CHAPTER 1

RESULTS

MOs activity spontaneously recovers after MOp stroke

Recent rodent studies have demonstrated that non-dexterous forelimb function can recover spontaneously after damage to the primary motor cortex (MOp)[20,21]. Recovering spontaneously suggests that the underlying repair processes are activated as a part of the endogenous injury response. To characterize the progression of these processes, we first sought to establish the time course of spontaneous recovery by training head-fixed mice to unilaterally pull a horizontal lever past a threshold: a task where the central challenge does not require substantial dexterity (Fig. 1a-b)[17-19].

Next, using the photothrombotic stroke model, we found that photothrombosis of the MOp reduced the amplitude and number of rewarded movements, but did not significantly impact movement quality as measured through the trajectory of lever position as previously reported (Fig. 1c-j)[22]. This effect is unlikely an artifact of lesion or the surgery procedure as a separate cohort of mice that received sham or visual cortical (VISp) strokes did not exhibit similar deficits despite having similar infarct sizes. Importantly, mice were able to recover within 48-72 hours after stroke and recovery occurred independently of explicit training or task re-exposure as a separate cohort of mice not exposed to the task until 5 days post-stroke also recovered (Fig. 1k-n). Our results suggest that spontaneous recovery of non-dexterous forelimb function can occur within 72 hours after stroke.

We reasoned that the acute effects of stroke should be expressed at the peak of the behavioral deficits - prior to recovery, while chronic adaptations would be apparent after the animals had recovered. Previous studies claim that these adaptations could manifest as detectable

changes in neural activity patterns throughout the brain[5,16]. However, these interpretations are limited by the fact that many of these studies do not explicitly measure behavioral recovery, or they use stimulation-evoked maps from anesthetized animals: a preparation that does not reflect the endogenous neural activity of awake animals. Therefore, we examined the cortical activity of awake, behaving Thy1-GCAMP6s transgenic mice using widefield imaging (Fig. 2a-c)[18]. This approach allows us to simultaneously image large areas of cortical tissue to identify where and how neural activity patterns change after stroke.

In agreement with previous reports, we detected substantial activation of cortical networks coincident with the onset of movement (Fig. 2d-e)[18]. Focal photothrombosis of the MOp disrupted this activity pattern in the ipsilesional hemisphere - supporting the idea that focal perturbations can reverberate throughout the network and impact distal brain regions (Fig. 2g). Upon closer inspection, we also found that stroke causes a significant reduction in the magnitude of movement-aligned activity in the MOp, secondary motor cortex (MOs), and several adjacent sensory cortices (Fig. 2f). These regions are densely interconnected through excitatory axonal projections, and thus, are likely to be significantly impacted by the acute loss of MOp axons[23].

Coincident with spontaneous recovery, activity within the MOs is restored to that of pre-lesion levels (Fig. 2f). And surprisingly, these changes are accompanied by the re-emergence of cortical activation patterns remarkably like that of the pre-stroke pattern (Fig. 2g). Taken together, our results suggest that stroke transiently attenuates MOs activity, which is then restored to pre-lesion levels during recovery.

Inactivity of both excitatory and inhibitory MOs neurons after MOp stroke

Future attempts to leverage these findings into therapeutic interventions could be accelerated by characterizing the basis of the acute post-stroke inactivity. One possibility reflects

the unique contributions of inhibitory interneurons to dampen cortical activity: increased number and activity of inhibitory neurons or strengthening of inhibitory synapses[2,15,24]. An alternative possibility posits that since MOp neurons innervate both excitatory and inhibitory neurons in the MOs, denervation of MOp axons might affect all MOs neurons regardless of cell type[23].

To explore the basis of post-stroke inactivity, we separated excitatory and inhibitory neurons by co-transducing the MOs of VGAT-Cre transgenic mice with AAV-hSyn-GCAMP7f and AAV-DIO-mScarlet (Fig. 3a-c). With this approach, all neurons will express GCaMP7f but only VGAT+ inhibitory neurons will also express mScarlet. Although severe post-stroke edema prevented reliable registration of the same neurons over time, we did not notice a substantial difference in the number of neurons of either cell type (Fig. 3d). At the population level, both the initial post-stroke inactivity and subsequent activity restoration occurred similarly in both excitatory and inhibitory neurons (Fig. 3e, f).

Next, we considered whether post-stroke inactivity is caused by an increase in the strength of GABAergic synapses. Using ex vivo patch clamp electrophysiological recordings, we targeted visually identified CaMKII-expressing neurons did not detect any significant differences in the frequency or amplitude of spontaneous inhibitory postsynaptic currents (sIPSC) at the peak of the deficits - 1 day after stroke (Supplemental Fig. 1a, b). Together, our results suggest that post-stroke inactivity is not caused by an increase in the number or activity of GABAergic neurons or an increase in the strength of GABAergic synapses. Instead, both excitatory and inhibitory MOs neurons are equally affected by stroke which may reflect a tissue-wide effect.

Homeostatic synaptic plasticity in the MOs during spontaneous recovery

To elucidate the neural adaptations that are responsible for spontaneous recovery, we considered a prevailing assumption of stroke recovery - that lost function is remapped onto

surviving neurons[1]. Recent studies have shown that the activity of a large fraction of excitatory neurons are positively or negatively modulated by movement[25]. If lost function is remapped onto surviving neurons, then we might expect significant changes in the identity of these neurons (that is, positively or negatively modulated by movement), or changes in the population-wide activity pattern during movement. However, we did not observe a significant difference in the fraction of excitatory neurons classified as movement-related after recovery, nor did we observe a change in the population-wide activity pattern in the MOs (Fig. 3g-k, Supplemental Fig. 1). Based on the neurons we observe, our results suggest that spontaneous recovery reflects a homeostatic restoration of MOs activity rather than functional remapping.

Neurons can adapt to prolonged periods of inactivity by regulating the strength of its excitatory synapses[26]. To determine whether this occurs after stroke, we performed targeted whole-cell recordings from visually identified CaMKII-expressing neurons at different times after stroke (Fig. 4. a, b). We detected significantly larger and more frequent α-amino-3-hydroxy-5-methyl-4-isoxazolepropionic acid receptor (AMPAR)-mediated spontaneous excitatory postsynaptic currents (sEPSC) only after spontaneous recovery (Day 3) as determined by whole-cell patch clamp recordings at -70 mV (Fig. 4 c-e).

Of the multitudes of homeostatic plasticity mechanisms that strengthen excitatory synapses after prolonged inactivity, multiplicative synaptic scaling has been speculated to occur after stroke[1,26]. Through this process, the increased amplitude of AMPAR-mediated EPSC can be scaled by a single scaling factor and reflects cell-wide, synaptic adaptations. However, we did not find evidence to support multiplicative synaptic scaling (Fig. 4f). Instead, we found that the ratio of AMPAR to N-Methyl-d-aspartate receptor (NMDAR)-mediated EPSC (AMPAR/NMDAR ratio) significantly increases 3 days after stroke which indicates a synapse specific accumulation of

AMPAR (Fig. 4g, h). This synapse specific potentiation suggests that reparative processes can promote synaptic plasticity and may thereby enhance the therapeutic efficacy of rehabilitative training.

Activity-dependent NR2B expression is necessary for post-stroke plasticity

Previous studies have demonstrated that the enhancement of AMPAR-mediated transmission can be preceded by changes in the stoichiometry of synaptic NMDA receptors[10,12,13,27]. To determine whether stroke-induced neural inactivity in MOs recruits more NR2B-containing NMDAR into the synapse, we measured the fraction of NMDAR current blocked by the NR2B subunit antagonist, Ifenprodil (Fig. 5a-c). We found that stroke-induced inactivity of the MOs significantly increases the presence of NR2B subunit-containing NMDAR as early as 1 day after stroke (Fig. 5c, d). Note, that at this early time point, AMPAR-mediated sEPSC and AMPAR/NMDAR remain unchanged compared with controls suggesting that synaptic potentiation has yet to take place (Fig. 4d, e, h). Conversely, experimentally activating surviving MOs neurons should reduce the presence of NR2B-containing NMDAR. And so, we expressed the excitatory chemogenetic receptor hM3Dq in the MOs three weeks prior to stroke (Fig. 5a, b)[28]. One hour after stroke, we activated these neurons using intraperitoneal CNO injections and the next day, we observed that chemogenetic activation had reduced the presence of NR2B-containing NMDAR (Fig. 5c).

We reasoned that if NR2B signaling is indeed responsible for synaptic potentiation after stroke, sustained Ifenprodil pre-infusions should prevent the increase in AMPAR/NMDAR ratio. We subcutaneously implanted an osmotic pump to chronically deliver Ifenprodil immediately after stroke and performed ex vivo patch clamp recordings 3 days after stroke (Fig. 5e). Indeed, infusion of Ifenprodil prevented the stroke-induced increase in AMPAR/NMDAR (Fig. 5f).

In addition to a heightened state of neural plasticity, another key feature of the post-stroke critical period is an increase in the responsiveness to rehabilitative training in promoting the recovery motor dexterity[3,8 7]. If the plasticity mediated by enhanced NR2B signaling is indeed responsible for this training sensitivity, then sustained Ifenprodil infusions after stroke should interfere with training-dependent recovery of motor dexterity. It is well established that, unlike the spontaneous recovery of non-dexterous movements, the recovery of skilled prehension depends on rehabilitative training during the post-stroke critical period[2,3,7,29]. In agreement with previous findings using the skilled prehension task[2,3,29], we found that when daily training is initiated the day after stroke, animals were able to recover to baseline levels of performance within a week (Fig. 5g - i). However, blockage of NR2B-containing NMDAR or preventing the post-stroke period of inactivity with concurrent systemic infusions of Ifenprodil or CNO (to animals expressing hM3D in the MOs), respectively, prevented training-dependent recovery (Fig. 5g – i).

Experimental MOs inactivation restores the post-stroke critical period in an NR2B-dependent manner

Although rehabilitative training during the post-stroke critical period can facilitate recovery, training after this period has closed does not significantly improve functional outcomes[7,29]. Since we observed that activity-dependent, synaptic modifications in the MOs contribute to the heightened training sensitivity during the post-stroke critical period, we reasoned that experimental inactivation of the MOs even after this period should also enhance synaptic plasticity and restore training sensitivity.

To test this idea, we directly infused a voltage-gated sodium channel blocker, tetrodotoxin (TTX) or saline into the MOs of stroke-induced mice – long after the closure of the post-stroke critical period (21 days after stroke; Fig. 6a)[3]. It is well established that TTX can attenuate neural

activity for extended periods of time. The day after TTX infusions, we began retraining the animals on the skilled prehension task the day after injections and measured their accuracy in successfully grabbing pellets (Fig. 6b). Initially, animals injected with either TTX or saline performed similarly poorly compared to their pre-stroke performance (Fig. 6b). However, TTX injected mice quickly recovered to their baseline behavioral performance levels within a week, but saline injected mice remained unable to fully recover in the same period. This indicates that experimental inactivation by TTX restores a period of heightened training sensitivity.

Next, we examined whether TTX infusions can recruit more NR2B-containing NMDAR into the synapse. Whole cell recordings from adult, MOs neurons outside of the post-stroke critical period showed that neurons are largely insensitive to Ifenprodil; however, the day after TTX injections, neurons became markedly more sensitive to Ifenprodil. (Fig. 6c, d). If NR2B-mediated signaling were also responsible for this TTX-mediated restoration of heightened training sensitivity, then Ifenprodil administration would interfere with this TTX-induced plastic state. So, in another cohort of mice, 21 days after photothrombosis in MOp, we injected TTX into the MOs of animals implanted with an osmotic minipump to systemically infuse Ifenprodil or saline. In contrast to mice infused with saline, we find that mice infused with Ifenprodil were unable to recover dexterous motor skills despite equal amounts of prehension training (Fig. 6e). Taken together, our results suggest that experimental neural inactivation may restore the post-stroke critical period by increasing NR2B expression.

Figure 1. Spontaneous recovery of non-dexterous forelimb function after primary motor cortical stroke.

(A) Behavioral task schematic showing the task apparatus (top) and the structure of each trial (bottom); each 10 second trial is cued with an auditory cue and followed with a random intertrial interval of 8-15 seconds. Successfully pulling the lever during the trial is rewarded with ~4uL of water and proceeds to the next intertrial interval.

(B) Representative experimental timeline showing 7 days of pre-stroke training followed by 5 days of post-stroke recovery.

(C) Representative MOp infarct histology 5 days after stroke with cresyl violet staining. Scale bar 1mm.

(D) Quantitation of infarct size relative to the contralesional hemisphere (task exposure, n = 5; without task exposure, n = 5; VISp stroke, n = 5).

(E) Representative lever trajectories from the same mouse before stroke (day 0), after stroke (day 1), and after recovery (day 3).

(F) Representative trial-averaged lever trajectories from the same mouse. Data presented as mean (solid line) +/- SEM (shaded region).

(G) Relative fraction of rewards obtained compared to the number of rewards obtained before stroke.

(H) Average amplitude of rewarded movements.

(I) Average similarity of lever trajectories to baseline trajectory.

(J) Average trial-to-trial variation as measured by the variance of lever trajectories between trials.

(K) Relative fraction of rewards obtained compared to the number of rewards obtained before stroke without task exposure.

(L) Average amplitude of rewarded movements without task exposure.

(M) Average similarity of lever trajectories to baseline trajectory without task exposure.

(N) Average trial-to-trial variation as measured by the variance of lever trajectories between trials without task exposure.

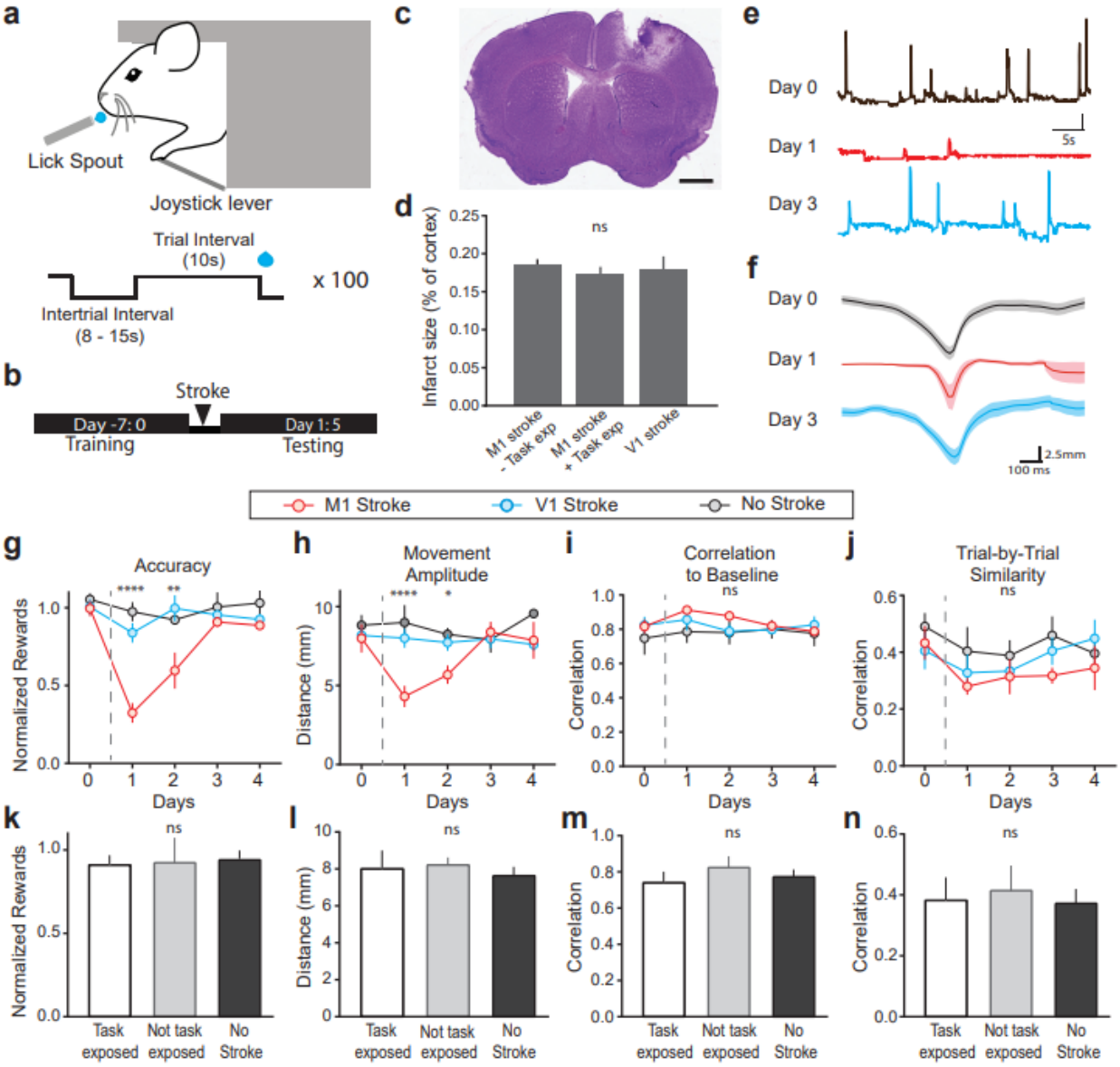
a
Lick Spout
Joystick lever
Trial Interval
(10s)
x 100
Intertrial Interval
(8 - 15s)
b
Stroke
Day -7: 0
Training
Day 1: 5
Testing
c
d
Infarct size (% of cortex)
ns
M1 stroke
- Task exp
M1 stroke
+ Task exp
V1 stroke
e
Day 0
Day 1
Day 3
5s
f
Day 0
Day 1
Day 3
2.5mm
100 ms
M1 Stroke
V1 Stroke
No Stroke
g
Accuracy
Normalized Rewards
Days
h
Movement
Amplitude
Distance (mm)
Days
i
Correlation
to Baseline
Correlation
Days
j
Trial-by-Trial
Similarity
Correlation
Days
k
Normalized Rewards
Task
exposed
Not task
exposed
No
Stroke
l
Distance (mm)
m
Correlation
n
Correlation

Figure 2. Cortex-wide cortical calcium dynamics recover to pre-stroke conditions coincident with spontaneous recovery

(A) Behavioral schematic showing the task apparatus with widefield imaging objective (left); representative image of dorsal cortical surface (right).

(B) Representative GCaMP signal from the MOp (top) and VISp (middle) with concurrent lever trajectory (bottom).

(C) Overlay of infarct from widefield images on atlas of dorsal cortex of all animals; increasing color intensity reflects the number of animals. Altas is modified from Allen Brain Atlas; numbers correspond to the legend in panel g.

(D) Representative trial-averaged example of dF/F from a single animal during the peri-movement period across the dorsal cortex.

(E) Representative trial-averaged example of dF/F from MOs and VISp. Red line indicates the onset of movement. Data presented as mean (solid line) +/- SEM (shaded region).

(F) Average of trial-averaged, peak amplitude of movement-related calcium signal across different brain regions (n = 7 animals); each color represents a different brain region. For each color, the triplet of bar graphs corresponds to day 0, 1, and 3 from left to right.

(G) Representative heatmap of normalized, trial-averaged, movement-related signals extracted from twenty-two brain regions on the ipsilesional hemisphere from one animal.

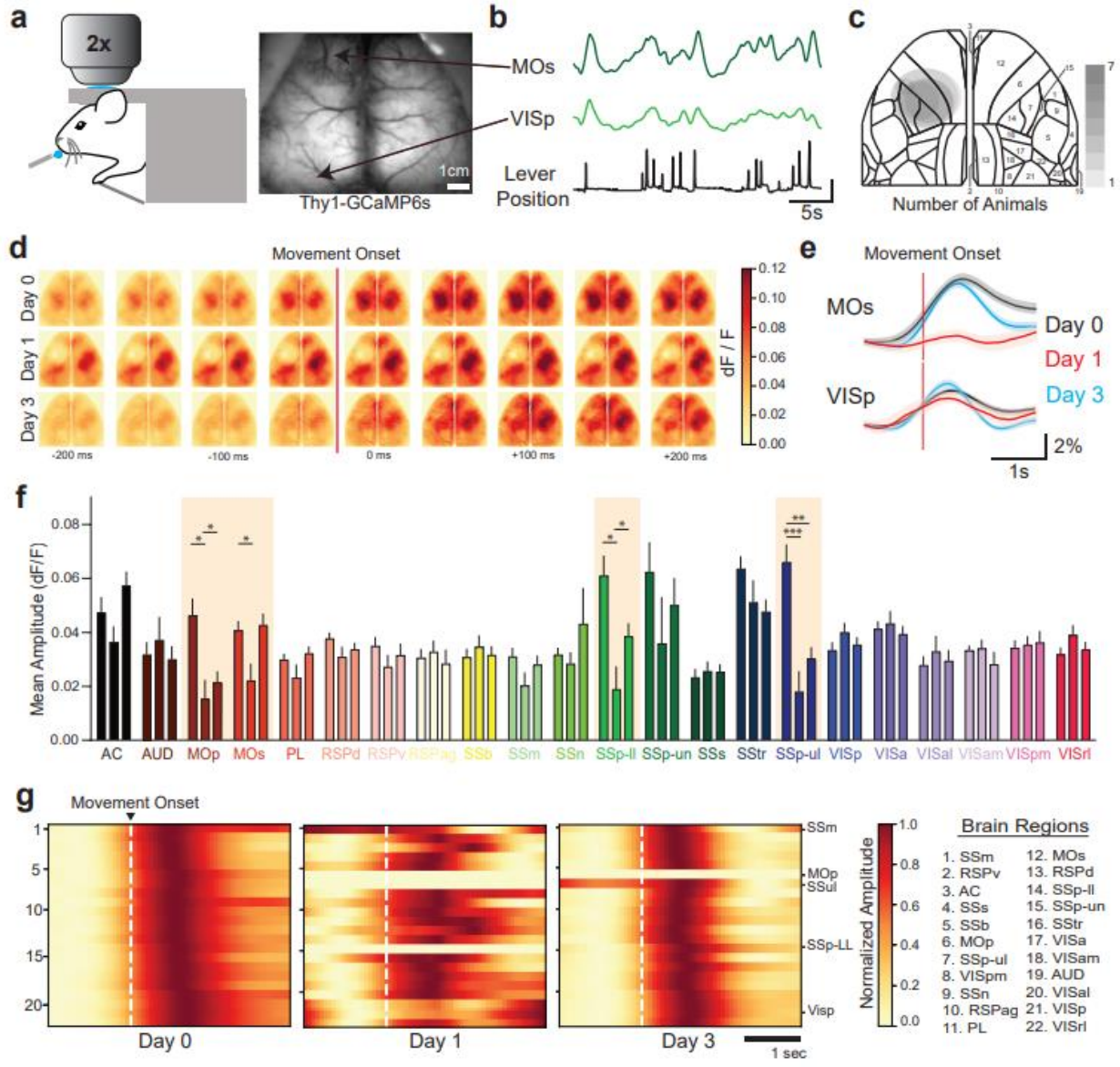
a
2x
1cm
Thy1-GCaMP6s
b
MOs
VISp
Lever Position
5s
c
Number of Animals
d
Movement Onset
Day 0
Day 1
Day 3
-200 ms
-100 ms
0 ms
+100 ms
+200 ms
dF / F
e
Movement Onset
MOs
VISp
Day 0
Day 1
Day 3
2%
1s
f
Mean Amplitude (dF/F)
AC AUD MOp MOs PL RSPd RSPv RSPag SSb SSm SSn SSp-ll SSp-un SSs SStr SSp-ul VISp VISa VISal VISam VISpm VISrl
g
Movement Onset
Day 0
Day 1
Day 3
1 sec
SSm
MOp
SSul
SSp-LL
Visp
Normalized Amplitude
Brain Regions
1. SSm
2. RSPv
3. AC
4. SSs
5. SSb
6. MOp
7. SSp-ul
8. VISpm
9. SSn
10. RSPag
11. PL
12. MOs
13. RSPd
14. SSp-ll
15. SSp-un
16. SStr
17. VISa
18. VISam
19. AUD
20. VISal
21. VISp
22. VISrl

Figure 3. Stroke induces pan-neuronal inactivity in the MOs.

(A) Schematic of viral injections. AAV-EF1a-DIO-mScarlet was mixed with AAV-EF1a-GCaMP7f and co-injected into the MOs of VGAT-Cre transgenic mice at the start of experiments. After training, mice received a photothrombotic stroke in the MOp.

(B) Representative image from 2-photon microscopy. While all neurons express GCaMP7f, only VGAT+ neurons expressed mScarlet.

(C) Representative GCaMP signal from pyramidal neurons (blue) and VGAT+ inhibitory neurons (red) and lever position (black, bottom). Rows of heatmap represent individual neurons, population averages are depicted below heatmap.

(D) Relative number of neurons detected between days does not significantly change after stroke.

(E) Normalized mean dF/F of individual neurons throughout the session significantly decreases after stroke, but recovers to baseline levels 3 days after stroke. Dashed line indicates stroke induction.

(F) Average number of detected events per second also significantly decreases after stroke, but recovers to baseline levels 3 days after stroke.

(G) Representative movement-aligned signals from two neurons: positively modulated (top) and negatively modulated (bottom). Fraction of positively and negatively modulated neurons does not differ before stroke and after recovery.

(H) Representative movement-aligned activity of individual neurons from a single animal.

(I) Movement-aligned population averages are not significantly different after recovery (representative individual animal, left; summary of all animals, right).

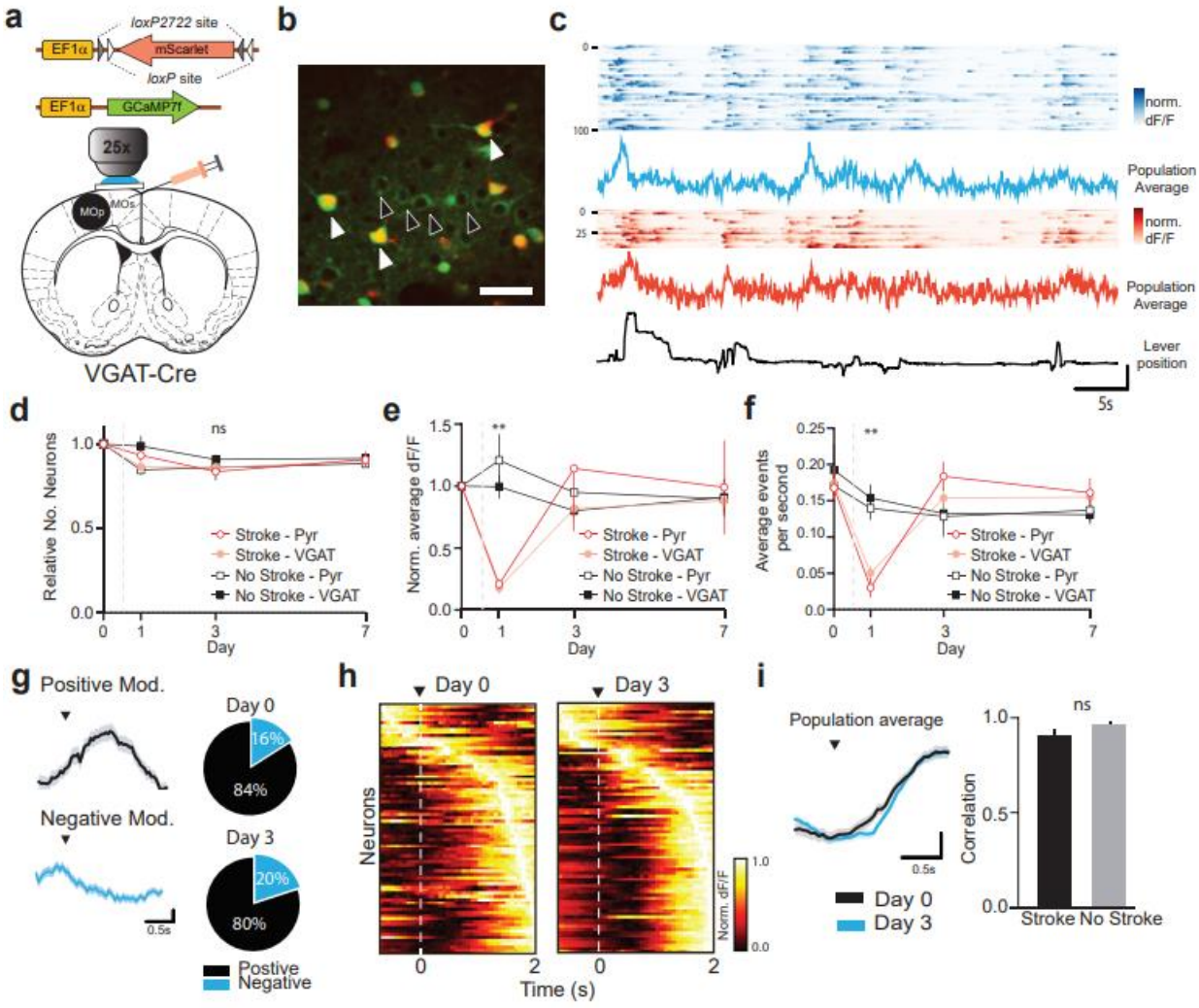
a
loxP2722 site
EF1α
mScarlet
loxP site
EF1α
GCaMP7f
25x
MOp
MOs
VGAT-Cre
b
c
norm. dF/F
Population Average
norm. dF/F
Population Average
Lever position
5s
d
ns
Relative No. Neurons
Stroke - Pyr
Stroke - VGAT
No Stroke - Pyr
No Stroke - VGAT
Day
e
**
Norm. average dF/F
Stroke - Pyr
Stroke - VGAT
No Stroke - Pyr
No Stroke - VGAT
Day
f
**
Average events per second
Stroke - Pyr
Stroke - VGAT
No Stroke - Pyr
No Stroke - VGAT
Day
g
Positive Mod.
Negative Mod.
0.5s
Day 0
16%
84%
Day 3
20%
80%
Postive
Negative
h
Day 0
Day 3
Neurons
Norm. dF/F
Time (s)
i
Population average
0.5s
Day 0
Day 3
ns
Correlation
Stroke
No Stroke

Figure 4. Increased synaptic potentiation three days after stroke.

(A) Schematic of viral injection strategy (left); MOs is injected with AAV-CaMKII-eGFP to express eGFP in excitatory, CaMKII expressing neurons. Representative DIC image from patch clamp recordings (right).

(B) Experimental timeline. Patch clamp recordings were made at days 0 (no stroke), 1, and 3.

(C) Representative traces of spontaneous, AMPAR-mediated EPSC (sEPSC) from whole-cell recordings from CaMKII-expressing MOs neurons.

(D) sEPSC amplitude from perilesional, MOs neurons. No Stroke (27 cells, 8 animals); Day 1 (26 cells, 8 animals); Day 3 (30 cells, 8 animals).

(E) sEPSC frequency from perilesional, MOs neurons. No Stroke (27 cells, 8 animals); Day 1 (26 cells, 8 animals); Day 3 (30 cells, 8 animals).

(F) Multiplicative synaptic scaling of sEPSC amplitude after recovery (red) and without stroke (unscaled: black; scaled: grey).

(G) Representative EPSC at -70mV and +40mV. Black marks indicate points taken to calculate AMPA/NMDA ratio (AMPA (-70mV): 5-10ms after stimulation; NMDA (+40mV): 50-55ms after stimulation). Scale bar, (No Stroke, 12pA; Stroke Day 1, 24pA; Stroke Day 3, 35pA).

(H) Summary of AMPA/NMDA ratios. No Stroke (14 cells, 5 animals); Day 1 (9 cells, 4 animals); Day 3 (18 cells, 6 animals).

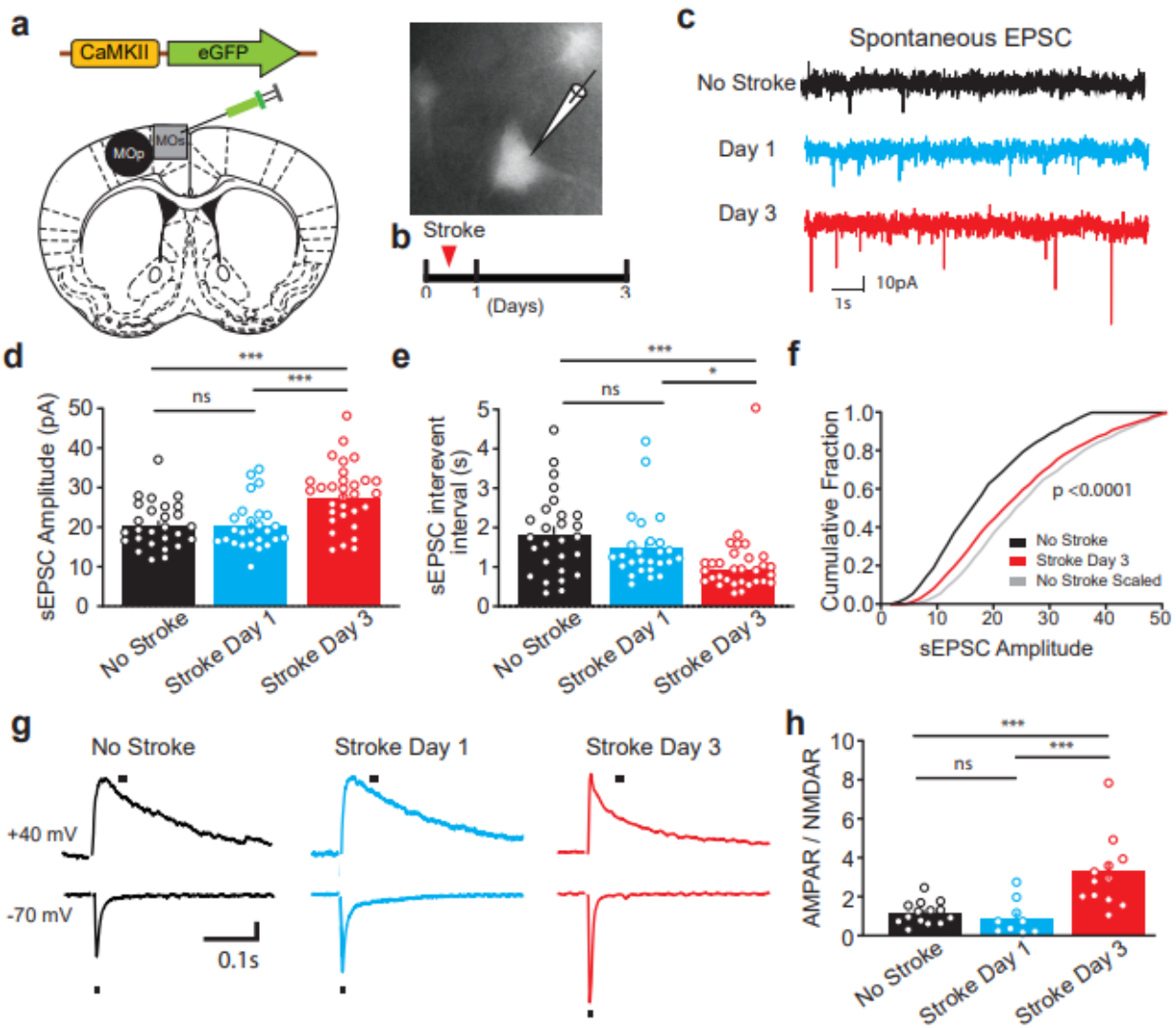
a
CaMKII
eGFP
MOp
MOs
b
Stroke
0
1
3
(Days)
c
Spontaneous EPSC
No Stroke
Day 1
Day 3
10pA
1s
d
sEPSC Amplitude (pA)
ns
***
***
No Stroke
Stroke Day 1
Stroke Day 3
e
sEPSC interevent interval (s)
ns
***
*
No Stroke
Stroke Day 1
Stroke Day 3
f
Cumulative Fraction
p <0.0001
No Stroke
Stroke Day 3
No Stroke Scaled
sEPSC Amplitude
g
No Stroke
Stroke Day 1
Stroke Day 3
+40 mV
-70 mV
0.1s
h
AMPAR / NMDAR
ns
***
***
No Stroke
Stroke Day 1
Stroke Day 3

Figure 5. Neuronal inactivity is necessary for NR2B-dependent recovery after stroke.

(A) Schematic of viral injection strategy; MOs is injected with AAV-EF1a-DIO-hM3D-mCherry and AAV-EF1a-Cre to label MOs neurons.

(B) Representative fluorescent image of injection site in MOs. Scale bar 1mm.

(C) Representative traces of NMDAR current before and after 30 minutes of bath application of Ifenprodil (3uM). Scale bar, (No Stroke, 68pA; Stroke Day 1 - saline, 171pA; Stroke Day 1 – CNO, 83pA),

(D) Summary of Ifenprodil sensitivity as measured by the normalized amplitude of NMDAR currents after Ifenprodil application. No Stroke (9 cells, 5 animals); Stroke Day 1 Saline (11 cells, 6 animals); Stroke Day 1 CNO (8 cells; 5 animals).

(E) Experimental timeline (top); Representative EPSC at -70mV and +40mV. Black marks indicate points taken to calculate AMPA/NMDA ratio (AMPA (-70mV): 5-10ms after stimulation; NMDA (+40mV): 50-55ms after stimulation). Representative traces taken from animals chronically administered with Ifenprodil (right). Scale bar, (Stroke Day 3 – saline, 42pA; Stroke Day 3 – Ifenprodil, 17pA).

(F) Summary of AMPAR/NMDAR from animals administered saline (8 cells, 5 animals) and Ifenprodil (14 cells, 5 animals).

(G) Schematic of skilled prehension experiment with timeline.

(H) Effects of chronic osmotic Ifenprodil infusion on recovery of the ability to grab and retrieve food pellets on the skilled prehension task (saline, n = 6; Ifenprodil, n = 6).

(I) Effects of chronic CNO infusions on recovery of the ability to grab and retrieve food pellets on the skilled prehension task (saline, n = 6; CNO, n = 6). Dashed line indicates stroke induction.

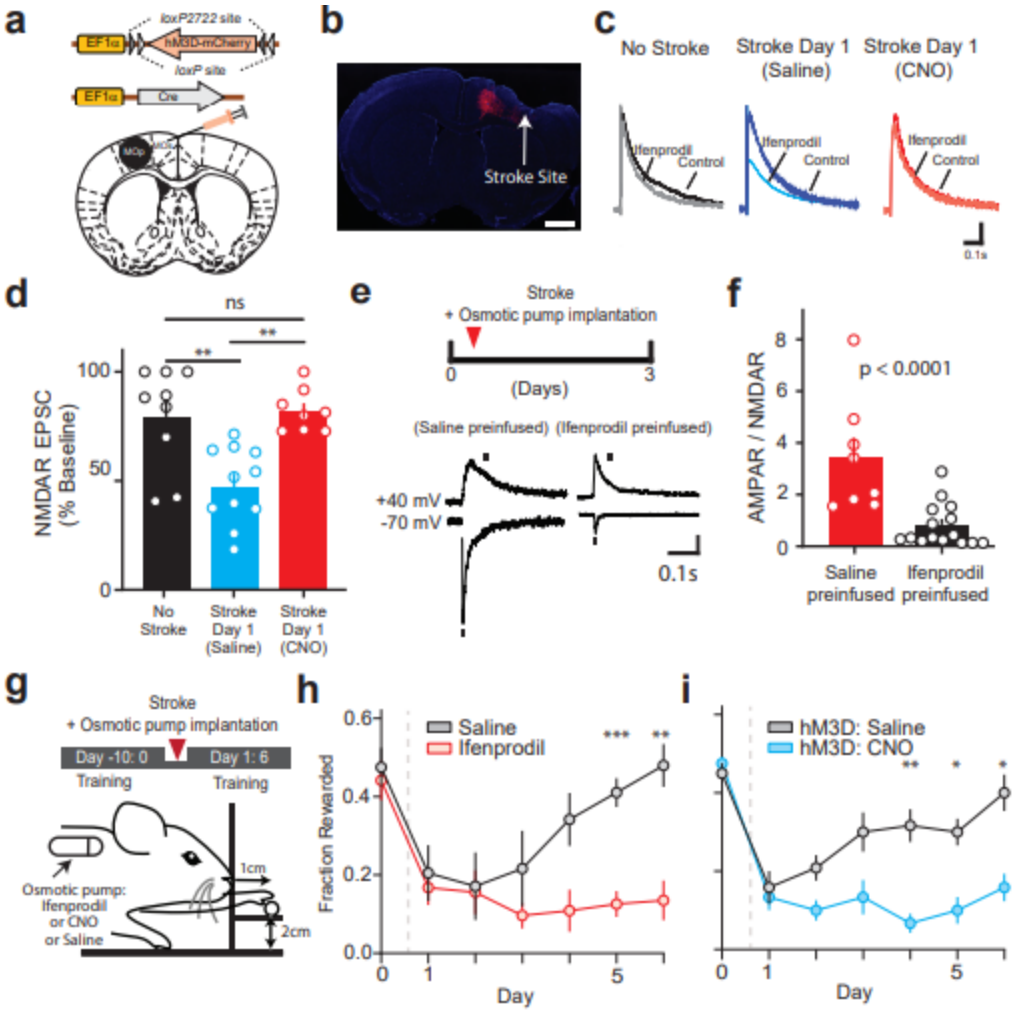
a
loxP2722 site
EF1α
hM3D-mCherry
loxP site
EF1α
Cre
mOp
mCx
b
Stroke Site
c
No Stroke
Stroke Day 1 (Saline)
Stroke Day 1 (CNO)
Ifenprodil
Control
0.1s
d
ns
**
**
NMDAR EPSC (% Baseline)
100
50
0
No Stroke
Stroke Day 1 (Saline)
Stroke Day 1 (CNO)
e
Stroke
+ Osmotic pump implantation
0
3
(Days)
(Saline preinfused)
(Ifenprodil preinfused)
+40 mV
-70 mV
0.1s
f
AMPAR / NMDAR
p < 0.0001
8
6
4
2
0
Saline preinfused
Ifenprodil preinfused
g
Stroke
+ Osmotic pump implantation
Day -10: 0
Day 1: 6
Training
Training
Osmotic pump: Ifenprodil or CNO or Saline
1cm
2cm
h
Saline
Ifenprodil
***
**
Fraction Rewarded
0.6
0.4
0.2
0.0
0
1
5
Day
i
hM3D: Saline
hM3D: CNO
**
*
*
0
1
5
Day

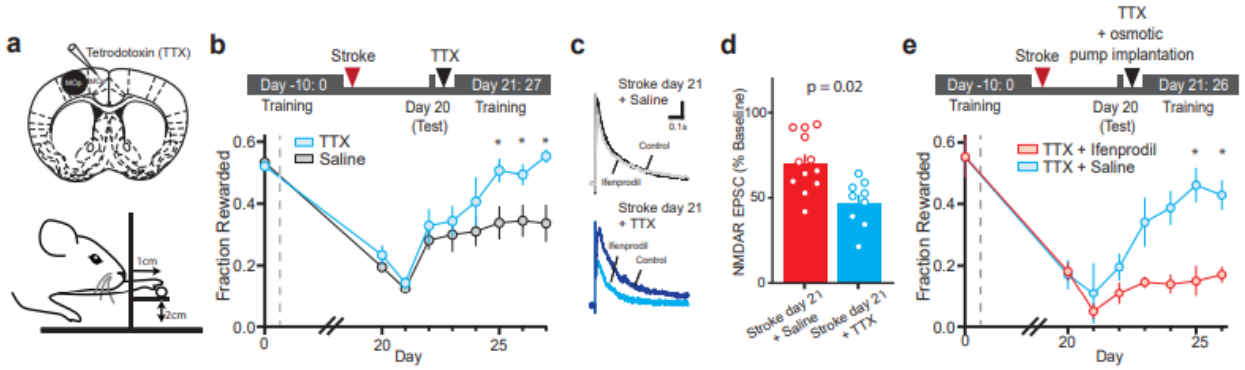

Figure 6. TTX infusions into MOs increases NR2B expression and restores heightened training sensitivity.

(A) Schematic of TTX injection strategy, behavior test (top, bottom, respectively). TTX was infused into the MOs three weeks after MOp stroke.

(B) The effects of TTX on recovery of forelimb function 21 days after stroke. Experimental timeline (top). Relative number of rewards obtained on each day. TTX was injected after testing on day 20. (saline, n = 8; TTX, n = 8).

(C) Representative EPSC at +40mV before and after Ifenprodil bath application. Scale bar, (Stroke Day 21 + Saline, 52pA; Stroke Day 21 + TTX, 21pA).

(D) Summary of the effects of 1 day of TTX injections on the Ifenprodil sensitivity assay. Saline injected (n = 13 cells, 5 animals); TTX injected (n = 10 cells, 5 animals).

(E) The effects of systemic Ifenprodil infusions on TTX-mediated recovery of forelimb dexterity. Experimental timeline (top). Relative number of rewards obtained on each day. TTX was injected and Ifenprodil-containing osmotic minipumps were subcutaneously implanted after testing on day 20 (saline, n = 5; Ifenprodil, n = 5). Dashed line indicates stroke induction.

Supplemental Figure. 1 | Changes in properties of movement-related excitatory M2 neurons after stroke.

(A) Average normalized dF/F responses for movement-aligned excitatory neurons after stroke. Each non-VGAT+ neuron was movement aligned (-1s : +2s) and the dF/F was averaged across trials. The dF/F from every neuron was then averaged per animal per day. The responses per animal was then normalized to that of the same animal on day 0.

(B) Fraction of all movement related neurons active during any given trial doesn't change . For each trial, each movement-related neuron was determined to be active or not (see methods). The fraction of all movement-related neurons per trial was then averaged across trials per session. Dashed line indicates stroke induction. All data presented as mean +/- SEM. *P < 0.05. NS, not significant.

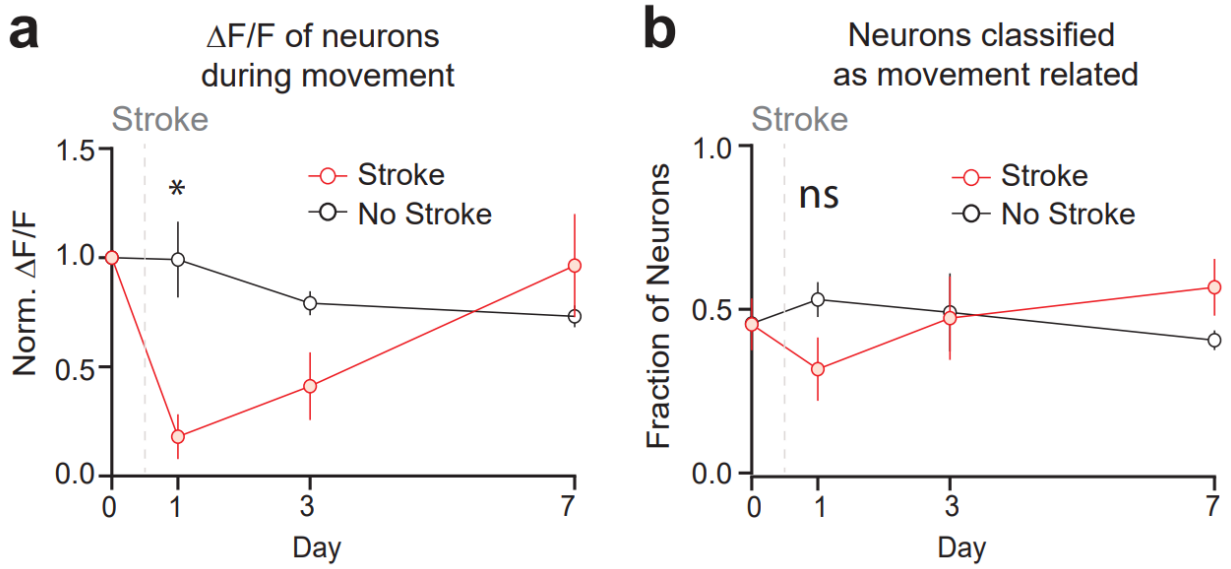
a
ΔF/F of neurons
during movement
Stroke
Norm. ΔF/F
1.5
1.0
0.5
0.0
*
Stroke
No Stroke
0
1
3
7
Day
b
Neurons classified
as movement related
Stroke
Fraction of Neurons
1.0
0.5
0.0
ns
Stroke
No Stroke
0
1
3
7
Day

Supplemental Figure. 2 | Lack of inhibitory synaptic changes in surviving M2 neurons.

(A) Voltage clamp recordings of spontaneous inhibitory postsynaptic current made from GFP-labeled M2 neurons held at 0mV. No Stroke (35 cells, 8 animals); Day 1 (28 cells, 7 animals); Day 3 (30 cells, 8 animals). Representative traces of spontaneous inhibitory postsynaptic current (sIPSC) from whole-cell recordings from CaMKII-expressing M2 neurons.

(B) sIPSC amplitude.

(C) sIPSC frequency. NS, not significant.

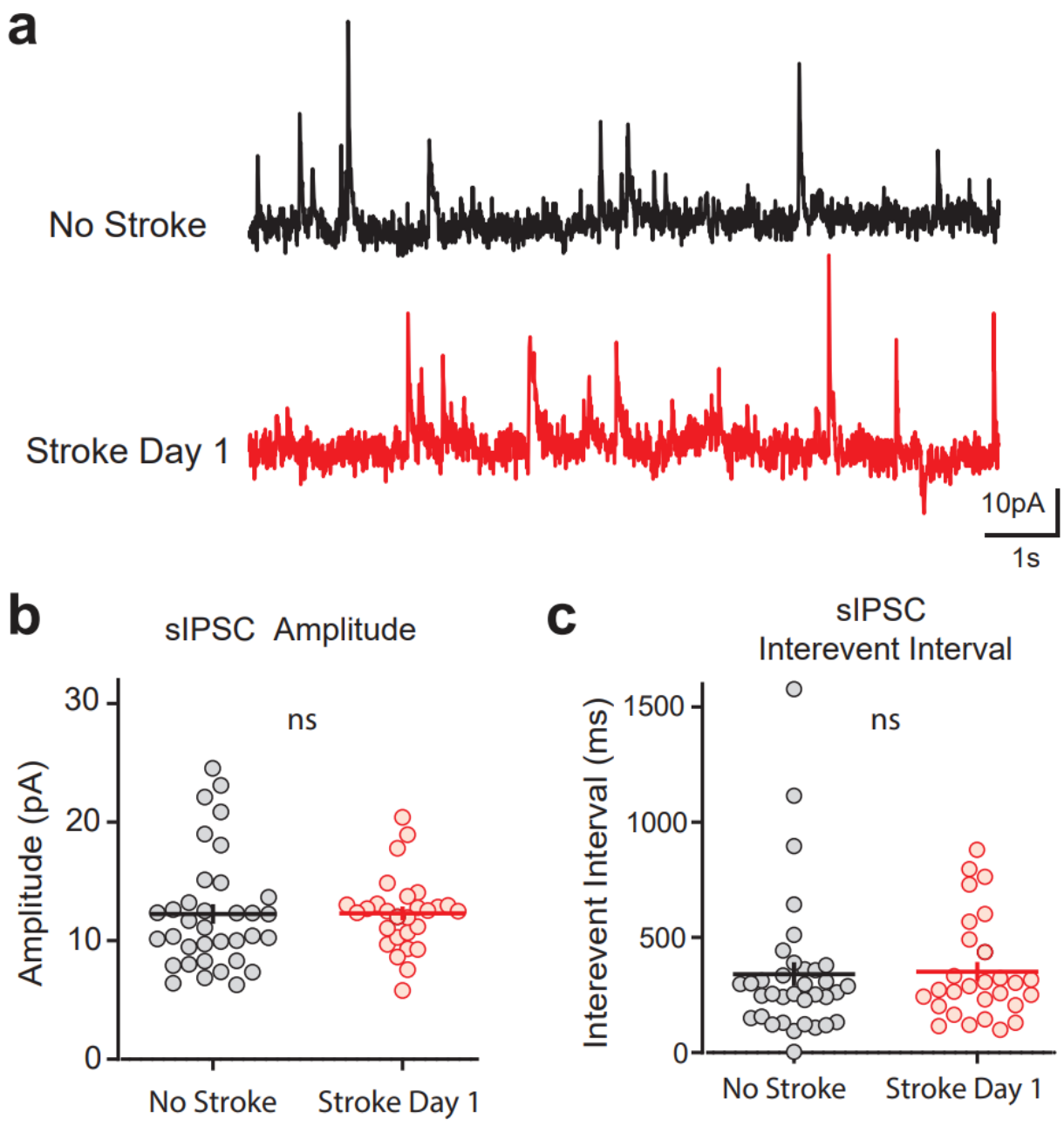
a
No Stroke
Stroke Day 1
10pA
1s
b
sIPSC Amplitude
ns
Amplitude (pA)
30
20
10
0
No Stroke
Stroke Day 1
c
sIPSC
Interevent Interval
ns
Interevent Interval (ms)
1500
1000
500
0
No Stroke
Stroke Day 1

Supplemental Figure. 3 | Cartoon depiction of proposed mechanism of post-stroke plasticity.

(A) Abstract network of dense recurrent connections (top three nodes) and feedforward to output (bottom).

(B) Focal lesions (top right node, gray) cause an acute loss of excitatory inputs to adjacent, surviving neurons (top middle node, black) and downstream neurons (bottom node, black).

(C) Persistent inactivity causes an increase in the expression of NR2B in inactive neurons (top middle node, white; bottom node, white)

(D) The presence of NR2B enables afferent synapses to more readily potentiate (red arrows). A possible prediction of this proposal is that increased NR2B expression and subsequent synaptic potentiation might also occur in areas that receive excitatory inputs from the M1 (eg. spinal cord, striatum, thalamus).

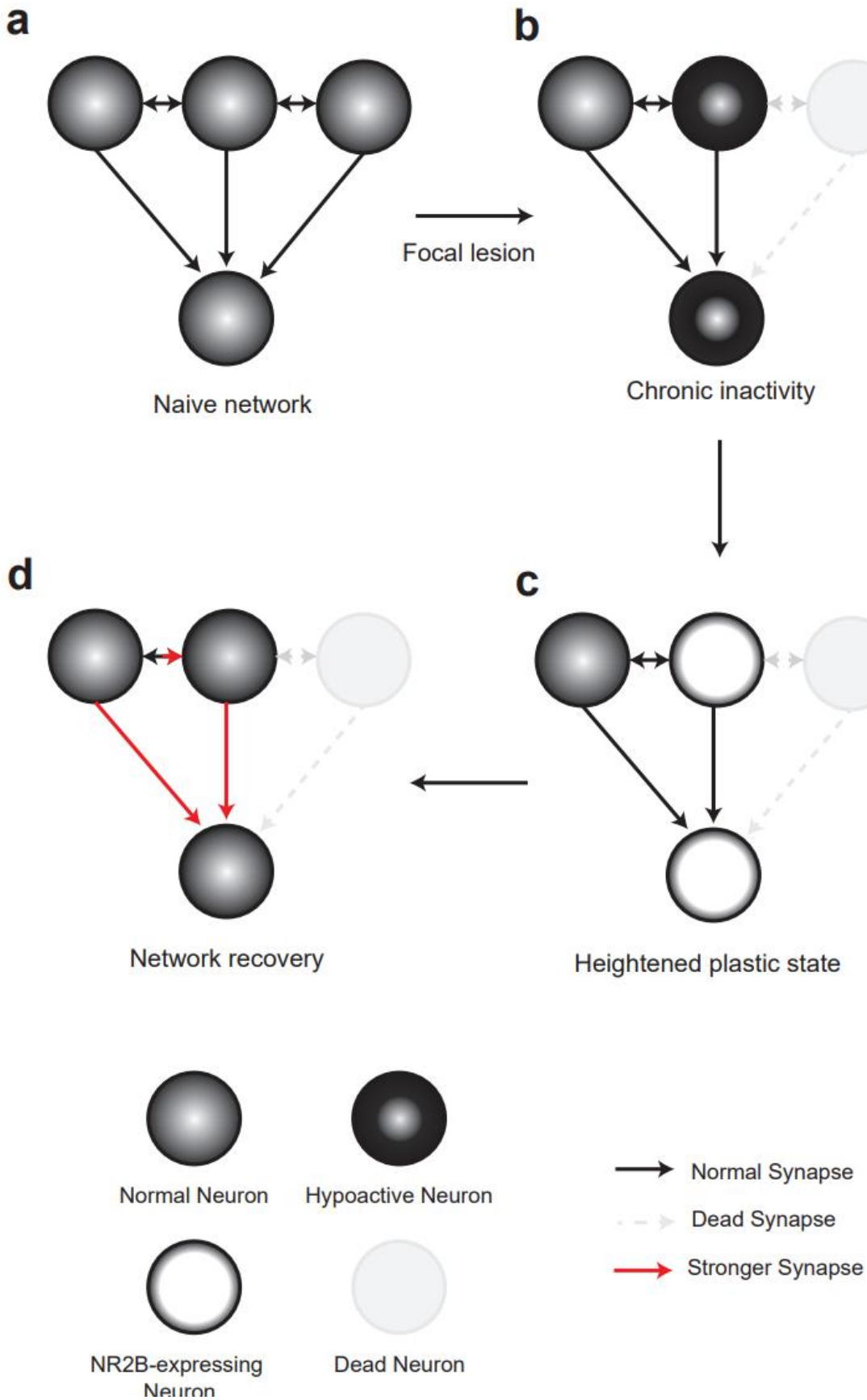
a
b
Focal lesion
Naive network
Chronic inactivity
d
c
Network recovery
Heightened plastic state
Normal Neuron
Hypoactive Neuron
NR2B-expressing Neuron
Dead Neuron
Normal Synapse
Dead Synapse
Stronger Synapse

Chapter 1, in full, is currently being prepared for submission for publication of the material. Wang, Eric; Lilascharoen, Varoth; Wang, Qingdi; Tran, Amanda; Yoon, Christopher; Honma, Patrick; Shu, Senling; Ro, Russell; Choi, Jun-Hyeok; Wang, Xiao-Yun; Knowland, Daniel; Lim, Byungkook. The dissertation author was the primary investigator and author of this material.

CHAPTER 2

DISCUSSION

Theodosius Dobzhansky once said that “nothing in biology makes sense except in the light of evolution”. Understanding how the brain adapts to injuries such as stroke is no different. It might be easier to understand the processes of neural repair and neuro-regeneration if we had an idea of how and why it evolved. From there, we may be better positioned to design and develop therapies to improve stroke recovery.

The ability to adapt to perturbations is extremely well conserved in all living things. The fact that the non-living components of organisms (eg. biomolecules) also exhibit the ability to adapt raises the possibility that adaptation is a key feature that gives rise to life itself. Consider just prior to the dawn of life on Earth where stochastic chemical processes led to the formation of new compounds. A critical step in the evolution of life was the emergence of autocatalytic sets: closed-loop chemical reactions. These reactions exhibited two key properties: metabolism, the ability to resynthesize its own components, and replication, the ability to produce more copies of itself. The evolution of autocatalytic sets is incredibly important as it 1) creates a self-sustaining system that is resilient to external perturbations, and 2) it distributes the importance of an entity to multiple elements. That is, even if one critical compound is defunct, there are others that can take its place.

From this perspective, most, if not all, selection pressures favor system properties that help maintain a stable autocatalytic loop. For example, an equally important development was the emergence of enclosed membranes around autocatalytic reactions – providing an additional level of buffering from the extreme volatility of the early planet. Other examples of these properties are access to nutrients – molecules used in these autocatalytic reactions. And thus, evolved the ability to detect external nutrient levels and respond to low nutrient states by moving around more to a

point of higher nutrient concentration. A critical point in this process is the emergence of negative feedback loops that maintain a setpoint.

In this example of a nutrient feedback loop, the entity (or organism) has processes to detect the current nutrient state which may then activate mechanisms that increase/decrease motility. However, nutrient state is not the only variable that is actively regulated by negative feedback. Other variables such as temperature, biophysical forces, and bioelectric activity can all be subject to active regulation. In considering negative feedback loops, two key parameters must be addressed: 1) the time it takes the system to detect the perturbation and engage feedback mechanisms, and 2) the magnitude of the feedback mechanism. For example, if the feedback for nutrient systems takes too long to activate, then the animal is more likely to starve before finding a new nutrient source. Similarly, if the magnitude of the feedback mechanism – say the degree of movement – is too small, then the animal is also more likely to starve before finding a new nutrient source. In contrast, if the magnitude were too great, then its possible that the animal would "overshoot" a desired location. Moreover, if the feedback delay were too fast, then its possible that the animal would leave a location before consuming all the available resource: suboptimal.

Theories of neuro-evolution posit that neurons and the nervous system evolved as means to control these feedback mechanisms more quickly and precisely. Electric potentials are fast and graded and thus enable animals to quickly turn on/off their motility mechanisms as well as precisely control the degree of movement. However, use of these electrical signals also required organisms evolve mechanisms to maintain and regulate bioelectric activity within a dynamic range. Some mechanisms operate quickly (eg. the coordinated activation of excitatory and inhibitory neurons; ~milliseconds) and others more slowly (eg. epigenetic modification and gene expression regulation of ion channels and receptors; ~days). Given that fast electrical signals

convey information about organism behavior/cognition, the regulatory feedback signals must occur at a different time scale than these faster signals to avoid crosstalk and interference.

An additional feature of the nervous system is the ability to hold memory; that is to retain information about a stimulus long after the stimuli has ended. The substrate of these memories is presumed to be stored in the strengths of synaptic connections so that the same incoming information is reliably routed to the same output (eg. muscle fibers). Learning is the process of altering the strengths of these connections (aka. synaptic plasticity) to optimize outcomes. However, this feature is not unique to the nervous system as *all* cells contain traces of prior events (eg. through changes in gene expression profile). A particularly interesting example of this occurs in the slime mold, P. polycephalum, a unicellular organism. Absent of a nervous system, these organisms can remember the location of a food source. It does so by releasing "softening agents" in the presence of food. These chemicals soften the walls of the cell's tubes, and thus, enables the tubes around the location of the food to greatly expand - imprinting the location of the food for extended periods of time. This is a form of learning writ large.

Importantly, if the slime mold were hungry, then it releases more of these softening agents in response to contact with food. That is, the magnitude of the feedback mechanism (eg. release of softening agents) can be modulated by experience and the organism's current state. Neurons in the mammalian nervous system exhibit a similar ability to modulate its synaptic plasticity. In response to prolonged periods of bioelectrical inactivity, neurons can dramatically change its gene expression profile to increase activity (the opposite for prolonged periods of hyperactivity). One of the ways that it can do so is by increasing the propensity for synaptic plasticity to occur in a process that is now known as metaplasticity: the plasticity of plasticity. This process bridges the processes of synaptic plasticity and homeostatic regulation of bioelectric activity. Moreover, it

occurs on a very slow time scale (~ days) when compared to the mechanisms implemented by traditional synaptic plasticity (~seconds). Knowing that metaplasticity may be the substrate by which neurons adapt to injury, next, we focus on the signal that induces metaplasticity: prolonged inactivity.

The primary and secondary motor cortices are reciprocally connected through excitatory synapses and share long-range axonal projections to similar subcortical areas[23]. This anatomical wiring predicts that damage to the MOp would deprive the MOs of normal, excitatory inputs, and together, the absence of MOp and reduced MOs excitation would deny the subcortical motor controllers of non-dexterous movements of a requisite amount of excitatory drive[20,21]. Surviving neurons can subsequently adapt to this lack of excitation by modifying the properties and molecular composition of excitatory synapses to restore neural activity[21,26,30,31]. Our results support this hypothesis as we find that, immediately after stroke, the surviving MOs tissue exhibits pan-neuronal hypoactivity, which later normalizes to pre-lesion levels. In this way, homeostatic regulation of neural activity can restore enough excitatory drive to downstream motor controllers and enable the "spontaneous" recovery of non-dexterous movements[20,21].

In contrast to the spontaneous recovery of non-dexterous motor function, the recovery of motor dexterity is training dependent. While the distinction between these two classes of movements likely reflects different motor control systems[20,21], we posit that they may be similarly affected by endogenous repair mechanisms. Specifically, we propose that homeostatic synaptic plasticity mechanisms can transiently reduce the synaptic potentiation threshold, enhance synaptic plasticity, and make neural circuits more sensitive to the instructive signals provided by experience[2,13,30-33]. Absent of explicit rehabilitative training, this plastic state would also allow residual neural activity to form and strengthen synapses[12,13]. These results complement previous

studies that show a dramatic increase in dendritic spine formation in the days following cortical stroke[1,32,33]. However, that motor dexterity does not recover even despite these adaptations suggests that it is the precise changes in synaptic connectivity, not just synapse number or synapse strength, that is important for functional gains[17,19]. Moreover, just as during motor learning, the initial increase in the number excitatory synapses may be critical to the re-acquisition of lost function but is unlikely to be important for the expression of recovered motor dexterity since, weeks later, spine density normalizes and becomes comparable to that of naive mice[17,19,32]. Another period prominent of elevated synaptic plasticity and sensitivity to experiences is during the developmental critical period[9,35]. Although it remains unclear whether injured neurons regress to a developmental state[36], we find that surviving neurons capture an important property of developing neurons: elevated NR2B expression[9]. The slow inactivation kinetics of NR2B-containing NMDAR allows more calcium influx, and thus, facilitates synaptic plasticity by reducing the synaptic potentiation threshold[8,10,12,13]. Importantly, we find that training-dependent recovery is critically dependent on NR2B signaling as the NR2B antagonist, Ifenprodil, blocks training-dependent recovery.

Maturing neurons replace NR2B subunits with the faster inactivating NR2A subunit and become less likely to potentiate[9]. We also observed a gradual decrease in NR2B expression coincident with the end of post-stroke training sensitivity. Moreover, since activity blockade of the adult visual system through prolonged dark rearing or TTX infusions transiently increases NR2B expression and can restore ocular dominance plasticity[34,37], activity blockade may restore post-stroke plasticity. Consistent with this idea, we found that TTX infusions into the perilesional tissue increases NR2B expression and restores post-stroke training sensitivity. It is worth mentioning that the *transience* of increased NR2B expression is likely important since constitutive

NR2B overexpression can lead to maladaptive behaviors[38], and therefore, other non-constitutive therapeutic strategies should be considered.

If indeed, there exists interesting parallels between developmental and post-stroke plasticity, then the decades of work on restoring developmental plasticity in adult mammals may be repurposed to promote stroke recovery. In support of this idea, NOGO-A antibodies, tonic GABAR antagonists, and BDNF overexpression have all been shown to effectively restore developmental ocular dominance plasticity and promote stroke recovery[15,39-45]. Here, we strike another parallel - chronic neural inactivity can restore ocular dominance plasticity and promote stroke recovery. Although these approaches are operationally distinct, they share a similar ability to enhance synaptic potentiation - suggesting that enhancing synaptic potentiation may be a key node in stroke recovery.

It is worth discussing that at first glance, our results may seem to contradict past findings: inactivating neurons seem to both impair and improve function. However, this highlights an important distinction between mechanisms necessary for the recovery process versus the execution of recovered movements. Movement execution is unequivocally dependent on neuronal activity as acute activity blockade impairs motor function[18,19,21]. However, we find that chronic activity blockade can also prime the brain to recover if subsequent training experience is provided. This is evidenced by the fact that TTX infusions acutely worsens forelimb dexterity, but after the effects of TTX wear off, TTX-treated animals can recover more than their saline-treated counterparts.

Axonal sprouting is widely believed to be necessary for recovery, so our results may seem incompatible with previous studies that have shown that TTX infusions reduce sprouting after stroke[4]. However, that recovery can be observed without increased axonal sprouting suggests that, with sufficient residual axon fibers, insufficient sprouting may not be the limiting factor for

recovery in mice[46]. Instead, we consider the possibility that TTX enhances synaptic plasticity by altering the composition of excitatory synapses. This plastic state then serves as a permissive environment for motor training to rewire surviving neurons into functional circuits and induce training-dependent recovery.

In sum, we find that primary motor cortical stroke inactivates surviving neurons in the adjacent secondary motor cortex (Supplemental Fig. 3). Over time, inactive neurons adapt by modifying the subunit composition of excitatory synapses to include more NR2B-containing NMDA receptors. The biophysical properties of these receptors would allow synaptic potentiation to occur more readily, and in theory, would allow training to more effectively rewire neural circuits and promote functional recovery. Although NR2B expression gradually declines over time, we find that experimental neural inactivation through TTX infusions can increase NR2B expression and enhance training sensitivity. We hope that our results will inspire leveraging the decades of progress in restoring ocular dominance plasticity, such as through chronic fluoxetine administration, into stroke therapies[29,47,48].

Chapter 2, in full, is currently being prepared for submission for publication of the material. Wang, Eric; Lilascharoen, Varoth; Wang, Qingdi; Tran, Amanda; Yoon, Christopher; Honma, Patrick; Shu, Senling; Ro, Russell; Choi, Jun-Hyeok; Wang, Xiao-Yun; Knowland, Daniel; Lim, Byungkook. The dissertation author was the primary investigator and author of this material.

CHAPTER 3

MATERIALS AND METHODS

Animals

All procedures to maintain and use mice were approved by the Institutional Animal Care and Use Committee (IACUC) at the University of California, San Diego. Mice were maintained on a 12-hour light/dark cycle with regular mouse chow and water available *ad libitum* except when placed under food restriction. All behavioral experiments were performed during the light cycle. Thy1-GCaMP6s (JAX 024275) and VGAT-Cre (JAX 014548) transgenic mice were obtained from Jackson Laboratory and were maintained on a C57BL/6J background. For all experiments, male and female heterozygous mice aged 12-24 weeks were used.

Viral vectors

All AAV vectors used in this study were packaged as serotype DJ and generated as previously described. In brief, AAV vectors were produced by transfection of AAV293 cells (Agilent) with three plasmids: an AAV vector plasmid carrying target constructs. AAV helper plasmid (pHELPER; Agilent), and AAV rep-cap helper plasmid (pRC-DJ, gift from M. Kay). At 72 h post-transfection, the cells were collected and lysed by a repeated freeze-thaw procedure. Viral particles were then purified by an iodixanol step-gradient ultracentrifugation and subsequently concentrated using a 100-kDa molecular cutoff ultrafiltration device (Millipore). The genomic titer was determined by quantitative PCR. The AAV vectors were diluted in PBS to a working concentration of approximately 10^{13} viral particles/ml. The constructs used in this study were: AAV-hSyn-DIO-hM3D, AAV-hSyn-DIO-GFP, AAV-EF1a-GCaMP7f, and AAV-EF1a-DIO-mScarleti.

Stereotaxic surgeries

Mice were anesthetized with an intraperitoneal injection of ketamine (100 mg/kg) and dexmedetomidine (1 mg/kg). Animals were then placed onto a stereotaxic frame (David Kopf Instruments) after unresponsive to toe pinch, and were administered ophthalmic ointment. The body temperature was maintained with a heating pad during surgery and recovery from anesthesia. After shaving of the scalp and application of antiseptics, a vertical incision was made from the animals' ears to eyes to expose the skull. Brain position was adjusted until bregma and lambda were brought towards the same plane, and a unilateral craniotomy was performed on the coordinates above the cortex until the dura was exposed. All stereotactic coordinates were derived from Paxinos and Franklin mouse brain atlas.

Unless otherwise mentioned, viruses or TTX were infused into the brain by using pulled glass micropipettes coupled with a syringe pump (P.H.D ULTRA; Harvard Apparatus) at a rate of 100-150 nl/min. The secondary motor cortex coordinates were (AP: 0.5mm, ML: 1.0mm, DV: -0.7; AP: 2.0mm, ML: 1.0mm, DV: -1.0; AP: 2.0mm, ML: 2.5mm, DV: -1.0). Dorsoventral coordinates were measured from the dura surface. The needle was then withdrawn at a rate of 1mm/min, and then the burr hole was sealed with bone wax and incision sutured. Anesthesia was reversed by administering 0.05mL of atipamezole (antisedan) and SR Buprenorphine (0.5-1mg/kg) and Carprofen (5mg/kg) for analgesia.

Photothrombosis

Mice were anesthetized with Isoflurane and prepped in the same way as during stereotaxic injections (see above). Instead of drilling a hole into the skull, the skull above the primary motor cortex (AP: 0.5, ML: 1.75) was carefully thinned as much as possible - at least until brain blood vessels were readily visible. Rose Bengal (Sigma 330000) was injected intraperitoneally and allowed 5 minutes to circulate into the brain. A green LED (560nm) illuminated the surface of the

skull to induce photothrombosis for 15 minutes[2,3,29]. Incisions were sutured and mice were given Carprofen (5mg/kg) for analgesia.

To affix titanium head-plates to the skull, mice were prepared as during stereotaxic injections. After exposing the skull, a 19G needle was used to gently score the surface of the skull. A titanium head-plate was affixed to the skull and held in place with Metabond (Parkell 375-0407) for 15 minutes. The remainder of the incision was sutured and the mice were given analgesia.
For the cortex-wide widefield imaging experiments, mice were prepared as during the head-plate implantation surgeries except that a circular piece of scalp was removed to expose the entirety of the dorsal cortex. After the surface of the skull was scored and the head-plate secured, the remainder of the exposed skull was carefully thinned as much as possible - at least until the brain's blood vessels were readily visible. KrazyGlue (KG925) was carefully applied to the surface of the thinned skull and allowed to dry for 15 minutes. Analgesic was given after surgery.

For cranial window surgeries, a small patch of skin on the skull was shaved and disinfected, and then removed. To realize Ca^{2+} imaging and stoke procedures, a 4-mm-diameter craniotomy was performed over the left MOs and MOp cortex (centered ~1.5 mm anterior to the bregma and ~1.4 mm left of the midline). Mice were microinjected (100 nl/min) with 500 nl of a 1:1 mixture of AAV-syn-GCaMP7f and AAV-DIO-mScarlet in the MOs cortex (A/P: +1.6 ~ +1.8 mm, M/L: -1.1 ~ -1.3 mm, D/V: -0.7 mm). To seal the opened skull and achieve a chronic cranial window, 3 layers of 4 mm diameter glass cover slips (Warner Instruments) affixed to the bottom of a 5 mm diameter glass cover slip (Warner Instruments) were inserted into the opening in the skull and fixed with Metabond. A custom titanium head-plate was affixed to the skull.

Osmotic pump implantation

Mice were anesthetized with an intraperitoneal injection of ketamine (100 mg/kg) and dexmedetomidine (1 mg/kg). After shaving and applying antiseptics onto the scapula opposite the dominant limb (eg. left side for right handed mice), animals were placed onto a sterile surgery station. A vertical incision was made just above the scapula. Membrane underneath the skin was carefully dissected using forceps and a sterile osmotic pump (Alzet 2001) prefilled with 200uL Ifenprodil (10mg/kg) was inserted into the mouse. The incision was then sutured and anesthesia was reversed by administering 0.05mL of atipamezole (antisedan). Mice received subcutaneous injections of Carprofen (5mg/kg) for analgesia.

Head-fixed lever pulling task

After recovering from head-plate implantation, we restricted mice to 1mL of water every day. For 3 days, mice were placed onto the head-fix apparatus and allowed to habituate for 5-15 minutes per day. The head fix apparatus is a custom 3D printed design and held in place with alligator clips for all experiments with the exception of 2-photon imaging. The lever was a playstation joystick fitted with a custom 3D printed attachment piece and a galvage needle (PetSurgical AFN1474S) and placed to the right hand side of the mouse. The output lever position was sampled every 20msec using Arduino Mega through custom software and was carefully calibrated and converted to lever position and displacement. 10 second trial intervals presented with a 10s sound cue (100Hz) and interleaved with 8-15s random intertrial intervals. Lever displacement exceeding 4mm during the trial interval were considered successful pulls and rewarded with ~4uL of water dispensed to a lick port place immediately in front of the mouse that is paired with a reward cue (1000 Hz). During experimental days, mice were subject to up to 100 trials or 30 minutes of head fixation, whichever came first. Training lasted for 7 days, and mice were subject to stroke the next day. Lever displacement was used as a proxy for forelimb

movement. Offline, lever positions were upsampled to 1KHz and used for comparison of forelimb trajectories across days. While Task exposed mice were subjected to daily testing after stroke, Not task exposed mice were left in their home cages.

For analysis, we used the 500ms around the peak of each movement bout. To account for small deviations in starting positions, we each time point from the average of the baseline period prior to movement onset. The peak amplitude of each trial was then averaged per session across animals to obtain Fig. 1h. Each session was then trial averaged to create Fig. 1f. The number of rewards obtained in a day was normalized to the rewards obtained on Day 0 prior to stroke (Fig. 1g). For each mouse, the average lever time series was compared to the average lever time series on Day 0 by Pearson's correlation (Fig 1i). Trial-to-trial similarity was measured by taking the average of Pearson's correlations between every trial in each session (Fig 1j).

Skilled prehension task

We restricted mice to 3 grams of food per day until they reached 80-85% of their baseline body weight. The animals were then habituated to animal handling and sucrose reward pellets. Following habituation, mice were placed into a clear acrylic box with a narrow opening (1cm x 9cm). Food pellets were placed 1cm away from the opening 0.5cm to the left or right of center depending on mouse limb preference. Limb preference was determined over a course of several days where the mice would be presented food pellets on both left and right sides and allowed to freely grab either pellet; limb preference was determined as the side that received 5 rewards. Mice were then trained for two weeks for 10 minutes or 20 reaches each day, whichever occurred first. Successful reaches were determined as reaches where the mice were able to smoothly grab the food pellet and return to feed position without knocking the pellet over. Contacting the food pellet, but failure to grab or return it were considered failed trials. Accuracy was calculated as the number

of successful reaches / the number of total reaches (failed + successful). After training, mice who failed to obtain 20% success rates during the training phase were excluded from the experiment. After two weeks of training, animals received a stroke in the MOp and one day to recover from surgeries. For experiments that measured the effects of endogenous post-stroke critical period, animals began retraining on the task immediately the next day for up to a week. During chronic experiments that measured the effects of TTX in restoring post-stroke critical period, animals began retraining on the task 20 day later for up to a week.

Widefield imaging

Widefield Ca^{2+} imaging was performed using a custom microscope. A 2x/0.08 NA objective (Olympus PlanApo N) was used for all widefield experiments with excitation at 470nm(Prizmatix Optogenetics-LED Blue) for GCaMP6s signal. Excitation and emission light were separated and filtered using a dichroic mirror (Semrock FF495-Di03-25x36) and (Thorlabs FB470-10), respectively, and finally detected using a CMOS camera (Hamamatsu C-13440-20CU) Head-fixed mice were placed underneath the microscope objective and the distance between objective and the surface of the mouse skull were manually centered and focused. A start TTL signal from the Arduino behavior system was sent to trigger camera start. This helped synchronize behavior and imaging. For each session, a series of 512pixels x 512pixels images were collected at 50ms and downsampled to 128pixels x 128pixels for 18000 frames and saved as TIFF.

Widefield data processing

After image acquisition, the averaged TIFF stack was manually aligned with the mouse brain atlas (Allen Brain Common Coordinate Framework v3) using custom image alignment software (Fig. 2a, c). This alignment also helped ensure that images were aligned between multiple imaging sessions. Subsequently, a mask of the brain atlas was applied to each frame to exclude

surrounding pixels. For each pixel, the pixel intensity was filtered using the Savitzky-Golay filter from the scipy package with a window length of 25 frames and an order of 2. f0 was determined as the 5^{th} percentile of the fluorescent intensity values 20 seconds before and after each time point. The initial and final 10 seconds were dropped excluded from the analysis. dF/F was then calculated as (f – f0) / f0 where f corresponds to each time point. The stroke area was visible in these fluorescent images, and so a circular mask was applied to the stroke and used to approximate the infarct location and size for each animal on Day 1 (Fig. 2c).

The pixel at the center of each brain region identified through the brain atlas was used to represent the signal from each brain region. The movement onset time obtained through Arduino was converted to frames and used to timestamp the onset of movement. The mean amplitude of dF/F was calculated as the average dF/F between 0 and 2s of movement onset averaged over trials (Fig. 2e, f). To account for changes in fluorescent intensity between brain regions, in Fig. 2g, we normalized dF/F of the signal from -1s to +2s of movement to the peak of the amplitude during that period. Each region was then sorted in ascending order based on the time it took to reach the amplitude peak for day 0. The same ordering was kept for subsequent days. Hemisphere-wide correlation patterns were calculated by taking the trial-average of each of these traces, concatenating each of these brain regions and compared with that of day 0 (template) using pearson's correlation.

Two-photon imaging

Ca^{2+} imaging was performed using a custom two-photon microscope with adaptive optics (AO). A 25X 1.05 NA objective (XLPlan, Olympus) was used for all two-photon imaging, with excitation at 970 nm (Ti:sapphire laser, MaiTai DeepSee, Spectra-Physics) for GCaMP7f signal and 1040 nm for mScarlet signal respectively. GCaMP7f and mScarlet signals were separated

through a dichroic beamsplitter (FF552-Di02, Semrock), delivered through a green emission filter (FF01-520/60-25, Semrock) and a red emission filter (FF01-596/83-25, Semrock) respectively, and finally detected by two different photomultiplier tubes (GCaMP7f: H7422PA-40, Hamamatsu; mScarlet: PMT1001, Thorlabs).

A deformable mirror (DM97-15, ALPAO) built in the microscope performed AO correction to compensate for the aberrations induced by multi-layer glass windows. To get an optimal correction pattern of the deformable mirror (DM), an indirect method based on signal intensity was applied. We put a multi-layer glass window on the top of the fluorescent solution and imaged through the window. With a gradient-descent algorithm, we optimized the amplitude of the different Zernike modes that form the pattern of DM to achieve the maximum of the average intensity of images. The obtained pattern was saved and sent to the DM before imaging to improve the image quality. ScanImage software (Vidrio Technologies) was used to control image acquisition. Images were acquired with a field of view of 500 X 500 um or 600 X 600 um (512 X 512 pixels), at 15 frames per second.

2-photon image analysis

Preprocessing: For each imaging session, two sets of files were saved corresponding to the two imaging channels: red (mScarlet) and green (GCaMP). After stroke, severe edema prevented reliable registration between sessions based on intensity, but the red channel was used whenever possible to align images between sessions. The red channel was used to create a binary mask based on its fluorescent intensity. The classification threshold was manually adjusted per session.

The CaImAn[49] algorithm was used to preprocess calcium signals from the green channel. In brief, the tiff stack was motion corrected, source separated, and deconvolved. The dF/F traces of individual cells were manually examined for quality control. Traces severely impacted by motion

artifacts or other unexplained artifacts were excluded from analysis. Finally, the location and morphology of each cell was manually confirmed with an average projection of the raw trace.

Analysis: A randomly selected 50 second interval was used to generate the representative Fig. 3c. All cells from an individual imaging session were separated into excitatory (blue) and inhibitory (red) using the red channel mask (see above). Each neuron's dF/F trace was normalized by maximum value within this interval and displayed as a heatmap or averaged between neurons and displayed as a population average trace.

The number of neurons detected in the green channel was normalized to the number of neurons detected at day 0 (Fig 3d). Individual calcium events were detected using the scipy signal function; the total number of events were divided by the duration of the entire imaging session to yield the average events per second per neuron. This was then averaged across neurons to generate Fig 3f. The average dF/F of each of these events was then averaged and normalized to that of Day 0 (Fig 3e).

For subsequent "movement-related" analysis, we focused on the dF/F activity during movement bouts (0.5 seconds prior to movement onset until 2 seconds after movement onset) of excitatory neurons. We classified a neuron as "movement-related" if its average activity was greater or less than 95% of a randomly shuffled control. To create the shuffled control, we randomly generated 1,000 time points to represent "pseudo movement onset times". For both real movement onset times and pseudo movement onset times, for every cell, we subtracted the average dF/F of the 500ms prior to movement onset from the activity throughout the entire bout. Subsequently, we only considered the real value of the peak (or trough) after movement onset: movement peaks. If the distribution of real movement peaks was greater than 95% of pseudo movement peaks, then the cell was considered positively modulated. In contrast, if the distribution

of real movement peaks was less than 95% of pseudo movement peaks, then the cell was considered negatively modulated (Fig 3g).

The activity of movement-related neurons for a single animal were trial-averaged, normalized to the maximum value and displayed as a heatmap (Fig 3h). Subsequently, the activity was averaged across all neurons to represent the average population of the neurons (Fig 3i). This population average was then compared with that of the population average on Day 0 using Pearson's correlation (Fig 3i).

Chemogenetics experiments

Clozapine-*N*-oxide (CNO; Enzo) was dissolved in water to obtain a stock concentration of 5 mg/ml and stored in small aliquots at -20°C. The working solution was freshly prepared before each use by diluting the stock with 0.9% saline to obtain a concentration of (0.5mg/mL). Mice were gently anesthetized under Isoflurane and Clozapine-n-oxide (5mg/kg) or 0.9% saline was administered intraperitoneally 15-30min prior to the start of experiments.

***Ex vivo* patch clamp electrophysiology**

Mice were anesthetized with isoflurane and transcardially perfused with ice-cold choline-based slicing solution, containing (in mM): 25 $NaHCO_3$, 1.25 NaH_2PO_4, 2.5 KCl, 7 $MgCl_2$, 25 glucose, 0.5 $CaCl_2$, 110 choline chloride, 11.6 sodium ascorbate, and 3.1 sodium pyruvate. Brains were carefully extracted and transferred to a chamber filled with the same solution on a vibratome (VT1200; Leica). Brains were sliced at 300 mm and incubated at 35°C for 15-20 min in recovery solution, containing (in mM): 118 NaCl, 2.6 $NaHCO_3$, 11 glucose, 15 HEPES, 2.5 KCl, 1.25 NaH_2PO_4, 2 sodium pyruvate, 0.4 sodium ascorbate, 2 $CaCl_2$, and 1 $MgCl_2$. Slices were maintained at room temperature for at least one hour until transferred to a recording chamber of an Olympus BX51WI upright microscope. The chamber was continuously perfused with artificial

cerebrospinal fluid (ACSF), containing (in mM): 125 NaCl, 25 $NaHCO_3$, 2.5 KCl, 1.25 NaH_2PO_4, 11 glucose, 1.3 $MgCl_2$, and 2.5 $CaCl_2$, maintained at 30 ± 2°C by a feedback temperature controller. Slicing solution, recovery solution, and ACSF were constantly bubbled with 95% O_2 and 5% CO_2. All compounds were purchased from Tocris or Sigma.

For all recordings, patch pipettes (3-5 MΩ) were pulled from borosilicate glass (G150TF-4; Warner Instruments) with a DMZ Universal Electrode Puller (Zeitz Instruments) and filled with appropriate intracellular solutions. Liquid junction potential was not corrected for any experiments. Neurons were visualized with differential interference contrast optics or epifluorescence (Olympus). Recordings were made with a MultiClamp700B amplifier and pClamp10 software (Molecular Devices). Data were low-pass filtered at 1 kHz and digitized at 10 kHz with a digitizer (Digidata 1440; Molecular Devices). Series resistance was monitored and cells that displayed > 30% change over the duration of recording were excluded.

Pipettes were filled with a Cs-based intracellular solution, containing (in mM): 115 Cs^+-methanesulphonate, 10 HEPES, 1 EGTA, 1.5 MgCl2, 4 Mg^{2+}-ATP, 0.3 Na^+-GTP, 10 Na_2-phosphocreatine, 2 QX 314-Cl, 10 BAPTA-tetracesium (295 mOsm, pH 7.35). Electrically-evoked excitatory postsynaptic postsynaptic currents (EPSCs) were recorded from identified neurons at -70 mV (for EPSCs). Spontaneous EPSC and IPSC were also recorded at -70 mV and 0 mV, respectively. For Ifenprodil sensitivity experiments, NMDAR currents were measured at +40mV. Ifenprodil (3uM) containing ACSF was slowly added into the bath and recordings were made again after 30minutes. For AMPA/NMDA ratio experiments, picrotoxin (50uM) was added to the ACSF, and AMPA and NMDA currents were measured at -70mV and +40mV, respectively.

Statistics

Statistical analyses were performed using Prism 8 (Graphpad Software). All statistical data can be found in figure legends with corresponding sample sizes. The sample sizes were chosen based on common practice in mouse behavioral experiments. All data were tested for normality with Shapiro-Wilk test. Then the appropriate parametric or non-parametric tests were applied. Correction for multiple comparisons was performed using Tukey's multiple comparison test. All statistical tests were two-tailed. Statistical significance levels were set at $*p < 0.05$, $**p < 0.01$, $***p < 0.001$, **** $p < 0.0001$. All data are presented as mean ± SEM.

Histology

After experiments were complete, mice were deeply anesthetized with isoflurane and were transcardially perfused with ice-cold 4% paraformaldehyde in PBS. Brains were carefully extracted and post-fixed in the same fixative at 4°C for at least 12 hours. Brains were sliced at 60 mm thickness with a vibratome (VT1000; Leica). Brain sections were mounted on glass slides (SuperFrost Plus; Fisher Scientific) or collected and stored in cryoprotectant (30% ethylene glycol, 30% glycerol in PBS) at -20°C for immunohistochemistry. Mounted slides were coverslipped with DAPI Fluoromount-G (Southern Biotech) and imaged with a 10x objective on an Olympus VS120 virtual slide microscope. Cresyl violet staining was performed by first briefly washing the slides in clean ddH2O, and then soaked in increasing ethanol concentrations (50-100%). Slides were submerged in cresyl staining solution in darkness for 2 minutes, air dried and cover slipped. Infarct size was determined to be (total contralesional cortex area - intact ipsilesional cortex area) / (total contralesional cortex area).

Chapter 3, in full, is currently being prepared for submission for publication of the material. Wang, Eric; Lilascharoen, Varoth; Wang, Qingdi; Tran, Amanda; Yoon, Christopher; Honma,

Patrick; Shu, Senling; Ro, Russell; Choi, Jun-Hyeok; Wang, Xiao-Yun; Knowland, Daniel; Lim, Byungkook. The dissertation author was the primary investigator and author of this material.

REFERENCES

Barria, A., and R. Malinow. 2005. 'NMDA receptor subunit composition controls synaptic plasticity by regulating binding to CaMKII', *Neuron*, 48: 289-301.

Biernaskie, J., G. Chernenko, and D. Corbett. 2004. 'Efficacy of rehabilitative experience declines with time after focal ischemic brain injury', *J Neurosci*, 24: 1245-54.

Bollu, T., S. C. Whitehead, N. Prasad, J. Walker, N. Shyamkumar, R. Subramaniam, B. Kardon, I. Cohen, and J. H. Goldberg. 2019. 'Automated home cage training of mice in a hold-still center-out reach task', *J Neurophysiol*, 121: 500-12.

Bridi, M. C. D., R. de Pasquale, C. L. Lantz, Y. Gu, A. Borrell, S. Y. Choi, K. He, T. Tran, S. Z. Hong, A. Dykman, H. K. Lee, E. M. Quinlan, and A. Kirkwood. 2018. 'Two distinct mechanisms for experience-dependent homeostasis', *Nat Neurosci*, 21: 843-50.

Brown, C. E., P. Li, J. D. Boyd, K. R. Delaney, and T. H. Murphy. 2007. 'Extensive turnover of dendritic spines and vascular remodeling in cortical tissues recovering from stroke', *J Neurosci*, 27: 4101-9.

Brown, C. E., C. Wong, and T. H. Murphy. 2008. 'Rapid morphologic plasticity of peri-infarct dendritic spines after focal ischemic stroke', *Stroke*, 39: 1286-91.

Carmichael, S. T., and M. F. Chesselet. 2002. 'Synchronous neuronal activity is a signal for axonal sprouting after cortical lesions in the adult', *J Neurosci*, 22: 6062-70.

Chakraborty, M., L. F. Chen, E. E. Fridel, M. E. Klein, R. A. Senft, A. Sarkar, and E. D. Jarvis. 2017. 'Overexpression of human NR2B receptor subunit in LMAN causes stuttering and song sequence changes in adult zebra finches', *Sci Rep*, 7: 942.

Chen, S. X., A. N. Kim, A. J. Peters, and T. Komiyama. 2015. 'Subtype-specific plasticity of inhibitory circuits in motor cortex during motor learning', *Nat Neurosci*, 18: 1109-15.

Chen, W. S., and M. F. Bear. 2007. 'Activity-dependent regulation of NR2B translation contributes to metaplasticity in mouse visual cortex', *Neuropharmacology*, 52: 200-14.

Chollet, F., J. Tardy, J. F. Albucher, C. Thalamas, E. Berard, C. Lamy, Y. Bejot, S. Deltour, A. Jaillard, P. Niclot, B. Guillon, T. Moulin, P. Marque, J. Pariente, C. Arnaud, and I. Loubinoux. 2011. 'Fluoxetine for motor recovery after acute ischaemic stroke (FLAME): a randomised placebo-controlled trial', *Lancet Neurol*, 10: 123-30.

Clarkson, A. N., B. S. Huang, S. E. Macisaac, I. Mody, and S. T. Carmichael. 2010. 'Reducing excessive GABA-mediated tonic inhibition promotes functional recovery after stroke', *Nature*, 468: 305-9.

Clarkson, A. N., J. J. Overman, S. Zhong, R. Mueller, G. Lynch, and S. T. Carmichael. 2011. 'AMPA receptor-induced local brain-derived neurotrophic factor signaling mediates motor recovery after stroke', *J Neurosci*, 31: 3766-75.

Erisir, A., and J. L. Harris. 2003. 'Decline of the critical period of visual plasticity is concurrent with the reduction of NR2B subunit of the synaptic NMDA receptor in layer 4', *J Neurosci*, 23: 5208-18.

Fong, M. F., D. E. Mitchell, K. R. Duffy, and M. F. Bear. 2016. 'Rapid recovery from the effects of early monocular deprivation is enabled by temporary inactivation of the retinas', *Proc Natl Acad Sci U S A*, 113: 14139-44.

Gambrill, A. C., and A. Barria. 2011. 'NMDA receptor subunit composition controls synaptogenesis and synapse stabilization', *Proc Natl Acad Sci U S A*, 108: 5855-60.

Gianfranceschi, L., R. Siciliano, J. Walls, B. Morales, A. Kirkwood, Z. J. Huang, S. Tonegawa, and L. Maffei. 2003. 'Visual cortex is rescued from the effects of dark rearing by overexpression of BDNF', *Proc Natl Acad Sci U S A*, 100: 12486-91.

Giovannucci, A., J. Friedrich, P. Gunn, J. Kalfon, B. L. Brown, S. A. Koay, J. Taxidis, F. Najafi, J. L. Gauthier, P. Zhou, B. S. Khakh, D. W. Tank, D. B. Chklovskii, and E. A. Pnevmatikakis. 2019. 'CaImAn an open source tool for scalable calcium imaging data analysis', *Elife*, 8.

He, H. Y., B. Ray, K. Dennis, and E. M. Quinlan. 2007. 'Experience-dependent recovery of vision following chronic deprivation amblyopia', *Nat Neurosci*, 10: 1134-6.

Hensch, T. K. 2005. 'Critical period plasticity in local cortical circuits', *Nat Rev Neurosci*, 6: 877-88.

Hiu, T., Z. Farzampour, J. T. Paz, E. H. Wang, C. Badgely, A. Olson, K. D. Micheva, G. Wang, R. Lemmens, K. V. Tran, Y. Nishiyama, X. Liang, S. A. Hamilton, N. O'Rourke, S. J. Smith, J. R. Huguenard, T. M. Bliss, and G. K. Steinberg. 2016. 'Enhanced phasic GABA inhibition during the repair phase of stroke: a novel therapeutic target', *Brain*, 139: 468-80.

Hooks, B. M., T. Mao, D. A. Gutnisky, N. Yamawaki, K. Svoboda, and G. M. Shepherd. 2013. 'Organization of cortical and thalamic input to pyramidal neurons in mouse motor cortex', *J Neurosci*, 33: 748-60.

Kawai, R., T. Markman, R. Poddar, R. Ko, A. L. Fantana, A. K. Dhawale, A. R. Kampff, and B. P. Olveczky. 2015. 'Motor cortex is required for learning but not for executing a motor skill', *Neuron*, 86: 800-12.

Kirkwood, A., M. C. Rioult, and M. F. Bear. 1996. 'Experience-dependent modification of synaptic plasticity in visual cortex', *Nature*, 381: 526-8.

Lee, M. C., R. Yasuda, and M. D. Ehlers. 2010. 'Metaplasticity at single glutamatergic synapses', *Neuron*, 66: 859-70.

Makino, H., C. Ren, H. Liu, A. N. Kim, N. Kondapaneni, X. Liu, D. Kuzum, and T. Komiyama. 2017. 'Transformation of Cortex-wide Emergent Properties during Motor Learning', *Neuron*, 94: 880-90 e8.

Maya Vetencourt, J. F., A. Sale, A. Viegi, L. Baroncelli, R. De Pasquale, O. F. O'Leary, E. Castren, and L. Maffei. 2008. 'The antidepressant fluoxetine restores plasticity in the adult visual cortex', *Science*, 320: 385-8.

Mdzomba, J. B., N. Jordi, L. Rodriguez, S. Joly, F. Bretzner, and V. Pernet. 2018. 'Nogo-A inactivation improves visual plasticity and recovery after retinal injury', *Cell Death Dis*, 9: 727.

Mohajerani, M. H., K. Aminoltejari, and T. H. Murphy. 2011. 'Targeted mini-strokes produce changes in interhemispheric sensory signal processing that are indicative of disinhibition within minutes', *Proc Natl Acad Sci U S A*, 108: E183-91.

Murphy, T. H., and D. Corbett. 2009. 'Plasticity during stroke recovery: from synapse to behaviour', *Nat Rev Neurosci*, 10: 861-72.

Nakayama, K., K. Kiyosue, and T. Taguchi. 2005. 'Diminished neuronal activity increases neuron-neuron connectivity underlying silent synapse formation and the rapid conversion of silent to functional synapses', *J Neurosci*, 25: 4040-51.

Ng, K. L., E. M. Gibson, R. Hubbard, J. Yang, B. Caffo, R. J. O'Brien, J. W. Krakauer, and S. R. Zeiler. 2015. 'Fluoxetine Maintains a State of Heightened Responsiveness to Motor Training Early After Stroke in a Mouse Model', *Stroke*, 46: 2951-60.

Otchy, T. M., S. B. Wolff, J. Y. Rhee, C. Pehlevan, R. Kawai, A. Kempf, S. M. Gobes, and B. P. Olveczky. 2015. 'Acute off-target effects of neural circuit manipulations', *Nature*, 528: 358-63.

Perez-Otano, I., and M. D. Ehlers. 2005. 'Homeostatic plasticity and NMDA receptor trafficking', *Trends Neurosci*, 28: 229-38.

Peters, A. J., S. X. Chen, and T. Komiyama. 2014. 'Emergence of reproducible spatiotemporal activity during motor learning', *Nature*, 510: 263-7.

Peters, A. J., J. Lee, N. G. Hedrick, K. O'Neil, and T. Komiyama. 2017. 'Reorganization of corticospinal output during motor learning', *Nat Neurosci*, 20: 1133-41.

Poplawski, G. H. D., R. Kawaguchi, E. Van Niekerk, P. Lu, N. Mehta, P. Canete, R. Lie, I. Dragatsis, J. M. Meves, B. Zheng, G. Coppola, and M. H. Tuszynski. 2020. 'Injured adult neurons regress to an embryonic transcriptional growth state', *Nature*, 581: 77-82.

Schabitz, W. R., T. Steigleder, C. M. Cooper-Kuhn, S. Schwab, C. Sommer, A. Schneider, and H. G. Kuhn. 2007. 'Intravenous brain-derived neurotrophic factor enhances poststroke sensorimotor recovery and stimulates neurogenesis', *Stroke*, 38: 2165-72.

Turrigiano, G. 2012. 'Homeostatic synaptic plasticity: local and global mechanisms for stabilizing neuronal function', *Cold Spring Harb Perspect Biol*, 4: a005736.

Urban, D. J., and B. L. Roth. 2015. 'DREADDs (designer receptors exclusively activated by designer drugs): chemogenetic tools with therapeutic utility', *Annu Rev Pharmacol Toxicol*, 55: 399-417.

Wahl, A. S., W. Omlor, J. C. Rubio, J. L. Chen, H. Zheng, A. Schroter, M. Gullo, O. Weinmann, K. Kobayashi, F. Helmchen, B. Ommer, and M. E. Schwab. 2014. 'Neuronal repair. Asynchronous therapy restores motor control by rewiring of the rat corticospinal tract after stroke', *Science*, 344: 1250-5.

Wang, L., J. M. Conner, A. H. Nagahara, and M. H. Tuszynski. 2016. 'Rehabilitation drives enhancement of neuronal structure in functionally relevant neuronal subsets', *Proc Natl Acad Sci U S A*, 113: 2750-5.

Wu, Z., Z. Guo, M. Gearing, and G. Chen. 2014. 'Tonic inhibition in dentate gyrus impairs long-term potentiation and memory in an Alzheimer's [corrected] disease model', *Nat Commun*, 5: 4159.

Ying, S. W., M. Futter, K. Rosenblum, M. J. Webber, S. P. Hunt, T. V. Bliss, and C. R. Bramham. 2002. 'Brain-derived neurotrophic factor induces long-term potentiation in intact adult hippocampus: requirement for ERK activation coupled to CREB and upregulation of Arc synthesis', *J Neurosci*, 22: 1532-40.

Zeiler, S. R., E. M. Gibson, R. E. Hoesch, M. Y. Li, P. F. Worley, R. J. O'Brien, and J. W. Krakauer. 2013. 'Medial premotor cortex shows a reduction in inhibitory markers and mediates recovery in a mouse model of focal stroke', *Stroke*, 44: 483-9.

Zeiler, S. R., R. Hubbard, E. M. Gibson, T. Zheng, K. Ng, R. O'Brien, and J. W. Krakauer. 2016. 'Paradoxical Motor Recovery From a First Stroke After Induction of a Second Stroke: Reopening a Postischemic Sensitive Period', *Neurorehabil Neural Repair*, 30: 794-800.

Zeiler, S. R., and J. W. Krakauer. 2013. 'The interaction between training and plasticity in the poststroke brain', *Curr Opin Neurol*, 26: 609-16.

Zemmar, A., O. Weinmann, Y. Kellner, X. Yu, R. Vicente, M. Gullo, H. Kasper, K. Lussi, Z. Ristic, A. R. Luft, M. Rioult-Pedotti, Y. Zuo, M. Zagrebelsky, and M. E. Schwab. 2014. 'Neutralization of Nogo-A enhances synaptic plasticity in the rodent motor cortex and improves motor learning in vivo', *J Neurosci*, 34: 8685-98.

Zhao, M. G., H. Toyoda, Y. S. Lee, L. J. Wu, S. W. Ko, X. H. Zhang, Y. Jia, F. Shum, H. Xu, B. M. Li, B. K. Kaang, and M. Zhuo. 2005. 'Roles of NMDA NR2B subtype receptor in prefrontal long-term potentiation and contextual fear memory', *Neuron*, 47: 859-72.